A

A Novel *Drosophila* Gene, *dunc-115,* Functions as a Putative Actin Cytoskeleton Regulator During Growth Cone Navigation

by

Melissa C. Garcia

A Dissertation Submitted to the Graduate Faculty in Biology in partial fulfillment of the requirements for the degree of Doctor of Philosophy, The City University of New York.

2003

UMI Number: 3083666

ProQuest Information and Learning Company
300 North Zeeb Road
P.O. Box 1346
Ann Arbor, MI 48106-1346

This manuscript has been read and accepted for the Graduate Faculty in Biology in satisfaction of the dissertation requirement for the degree of Doctor of Philosophy.

4.15.2003
Date

Chair of Examining Committee
Dr. Qi He, Brooklyn College

4.24.03
Date

Executive Officer
Dr. Richard L. Chappell

Dr. Ray H. Gavin, Brooklyn College

Dr. Charlene Forest, Brooklyn College

Dr. Jürgen Polle, Brooklyn College

Dr. Jessica Treisman, New York University Medical Center

Supervisory Committee

The City University of New York

Abstract

A Novel *Drosophila* Gene, *dunc-115*, Functions as a Putative Actin Cytoskeleton Regulator During Growth Cone Navigation

By

Melissa C. Garcia

Adviser: Professor Qi He

dunc-115, a *Drosophila* homolog of gene *unc-115* in *C. elegans*, has been identified and characterized. It is an alternatively spliced gene with at least three isoforms revealed in flies, *dunc-115l*, *dunc-115m* and *dunc-115s*, respectively and they have remarkable levels of conservation with other orthologs. Northern blot confirms the existence of multiple isoforms while *in situ* hybridization reveals a dominant expression in the CNS. Structurally, all three forms contain the LIM domains while only Dunc-115l possesses the villin head piece domain. Mutant analysis indicates that Dunc-115 proteins are pivotal mediators involved in the axonal navigation in both the visual system and the midline. Furthermore, the domain structure strongly implies a close association with the cytoskeleton network, which may play a role in guiding the axons.

Dedicated
to
My Mother

ACKNOWLEDGEMENTS

I would like to acknowledge my mentor Dr. Qi He for his professional input and his opinions, for which have aided me to grow.

I would like to thank Dr. R. H. Gavin for giving me access to his microscope and making me feel welcomed in his lab. I would like to thank him for his advice and for being a member on my committee.

Much thanks goes to my committee members Dr. Charlene Forest, Dr. Juergen Polle and Dr. Jessica Treisman for being extremely accommodating and reading this dissertation.

Additionally, I would like to thank the lab members. Anthony Bottalico who has been my lab mate for the past 4 years and he has been a source of support. Much thanks to the newest member, Chris Roblodowski who has been a great source of help.

Thanks to Dr. Catherine Mc Entee for advisement and support.

And on a more personal note I would like to thank my parents Rosita and Angelo Garcia, their love and support allowed me to continue to this level. I would also like to thank the rest of my family members, especially my sister Darlene and the youngest family member Cecilia for bringing love and laughter during the tough times. I would also like to thank my friends for their support.

TABLE OF CONTENTS

List of Tables

Chapter 2 Tables

Chapter 3 Tables

List of Figures

Chapter 1

Chapter 2

Chapter 3

Chapter 4

Chapter 5

Chapter 1. Introduction

I. Directed Outgrowth of Developing Axons

One primary goal of developmental neuroscience is to understand the cellular and molecular mechanisms that provide neurons with the ability to form accurate connections with their synaptic targets, and it is this selectivity that underlies the function of these circuits in the mature brain (Albright, 2000). There are four sequential steps in the development of neuronal circuits, namely, specification of distinguishable neuronal cell types, directed outgrowth of developing axons, selection of appropriate synaptic partners, and the refinement of connections (Albright et al., 2000; Goodman and Shatz, 1993)

During the construction of the central nervous system (CNS), developing neurons extend dendrites and axons in a highly stereotypic fashion. Among the early experiments were Roger Sperry's analyses showing that there was a high degree of precision in the topographic order of retinal axon projections in the amphibian visual system development (Sperry, 1963). Based on observations from this system, Sperry formulated the chemoaffinity hypothesis that stated the existence of a system of chemical labels between pre- and post- synaptic neuronal partners driving the selective synapse formation (Sperry, 1963; Albright, 2000).

The introduction of molecular biology into neuroscience has resulted in substantial progress since Sperry's theory and a more comprehensive model has emerged that emphasizes the existence of guidance cue gradients as positional information (Tessier-Lavigne and Goodman, 1996). Collectively,

there are four different types of guidance cues governing both attractive and repulsive axon pathfinding (Dickson, 2002; Tessier-Lavigne and Goodman, 1996). Thus the long-range repulsive and attractive cues function as gradients to repulse or attract axons, while the short-range repulsive and attractive cues require physical contacts with the incoming axons before they respond.

II. Growth Cone

The leading edge of a migrating axon is defined by the structure called the growth cone, which detects and responds to guidance signals in its surrounding environment. These signals navigate the growth cone to its specific synaptic target (Figure 1.1).

The growth cone consists of dynamic structures called filopodia and lamellipodia. Filopodia are spike-like projections that contain dense parallel actin bundles positioned with their fast growing end radiating toward the filopodia tips (Lewis and Bridgman, 1992;Wood and Martin, 2002). The filopodial surfaces contain guidance receptors as well as adhesion molecules that allow it to function in growth cone turning (Rochlin et al., 1999; Dickson, 2002), and thus the growth cone relies on filopodia for navigation instructions (Bentley and Toroian-Raymond, 1986; Steketee and Tosney, 2002). The filopodia have three different adhesive locations with specific functions at the shaft, tip, and base of the extension, respectively.

Upon binding to guidance cues, the filopodial tip adhesion initiates signals that modify the shaft adhesion that in turn regulates lamellipodial

advancement, while the basal adhesion functions in filopodial emergence (Steketee and Tosney, 2002). During navigation, the filopodia adopt a dynamic morphology through extending and collapsing mediated by nucleation, retrograde flow and extension of actin filaments (Dickson, 2002). It is unclear how filopodia are formed though one possibility is that they may come from lamellipodia actin bundles called microspikes (Small et al., 2002).

Interspersed between the filopodia are the lamellipodia, web-like structures defined by a network of loosely woven actin filaments and microspikes (Small et al., 2002). During growth cone navigation, the lamellipodia function in substrate adhesion, target recognition and leading edge advancing (Oledentbourg et al, 2000). Ultimately, the lamellipodial functions require the reorganization of the lamellipodium actin filament network.

The shaft of the growth cone contains cross-linked microtubule bundles that are involved in axon extension and growth cone turning (Dickson, 2002). As the growth cone navigates through its environment, it follows a trajectory characterized by choice points. A choice point is defined as the position where a threshold of guidance cues is achieved leading to a change in growth cone response (Dickson, 2002). Though the external cues are believed to steer axons by regulating the growth cone cytoskeleton, the signaling pathways involved remain largely elusive (Dickson, 2002).

III. Extrinsic Factors Involved in Growth Cone Navigation

i. Receptor Mediated Growth Cone Guidance

The four axon guidance mechanisms, chemoattractive, chemorepulsive, contact attractive, and contact repulsive, are conserved in the course of evolution (Dickson and Keleman, 2002). Several guidance molecules have been characterized in different species including the Netrins and the Slit-Robo pathways

a. The Netrins

The Netrins are bi-functional long-range guidance cues capable of mediating both attractive and repulsive responses (Hong et al., 1999; Dickson, 2002). Two types of Netrin receptors have been characterized that are conserved in worms, flies and vertebrates (Hedgecock et al., 1990; Kolodziej et al., 1996; Ackerman and Knowles, 1998). These receptors appear to be responsible for determining whether Netrins function as a repulsive or attractive cue.

The *C. elegans* Netrin homolog, Unc-6, is the first Netrin to be identified (Hedgecock et al., 1990). As the neuronal growth cones navigate circumferentially between the epidermis and the basal lamina in *C. elegans*, a subset of axons project dorsally while others send extensions out ventrally. Unc-6 forms a gradient along the dorsal-ventral ectodermal circumference with the highest concentration at the ventral midline and appears to be a key guidance cue (Wadsworth, 2002) (Figure 1.2). Subsequently, Unc-6 homologs have been identified in both vertebrates and *Drosophila*, where the name Netrin has been adopted (Harris et al., 1996; Serafini et al., 1994). Unlike in the worms, there are two forms of Netrins in vertebrates and flies.

Genetic analysis in *C. elegans* has revealed that Unc-40, genetically linked to Unc-6, is a receptor for Unc-6 (Hedgecock, 1990). Furthermore, the Unc-40 homolog has been found in the vertebrate as Deleted in Colorectal Carcinoma (DCC) (Chan et al., 1996), and in fruit flies as Frazzled (Kolodziej et al., 1996). More importantly, in all these species, Unc-40 appears to be associated with the axonal migration toward to the Netrin gradient (Chan, 1996; Mitchell, 1996; de la Torre, 1997). Thus, the Unc-6/Unc-40 pathway regulates proper ventral migration of pioneering axons in the CNS (Tessier-Lavigne, 1996, de la Torre, 1997, Kolodziej, 1996), suggesting the Unc-40 Netrin receptor is a principal mediator of the attractive effects of the Netrin proteins.

However, the finding that certain axons are repelled by the Netrin proteins implies a more complex and bifunctional role of these proteins (Colamarino and Tessier-Lavigne, 1995; Mitchell et al., 1996; Serafini et al., 1996). Further analysis reveals that the final outcome of the Netrin guidance cues is determined by the Netrin receptors. Thus, when Netrins bind to their receptor Unc-5 along with Unc-40, the responding axons carrying these receptors will receive the Netrin signal as repulsive and turn away (Colamarino and Tessier-Lavigne, 1995; Dickson and Keleman, 2002).

Collectively, one current model suggests that Unc-40 is a co-receptor for both the repulsive and attractive Netrin guidance cues. When Unc-40 is associated with Unc-5, the dimer mediates a repulsive response. If the

association is between Unc-40 and a yet unidentified co-receptor X, the complex will interpret Netrins as attractive cues (Giger and Kolodkin, 2000).

b. Slit

The Slit family constitutes another well conserved guidance mechanism across species (Brose and Tessier-Lavigne, 2000;Wong et al., 2002). In flies, the Slit protein functions as a midline repellent, where if the Slit protein is eliminated, axons will collapse as a result of the failure of axons leaving the midline (Guthrie, 1999; Kidd et al., 1999). One Slit receptor has been determined as Roundabout (Robo) (Guthrie, 1999).

There are three Robo isoforms: Robo1, Robo2 and Robo3. Robo1 appears to mediate short range repulsion in response to Slit, which prevents ipsilateral axons from crossing and commissural axons from recrossing the midline (Guthrie, 1999; Wong et al., 2002). Robo 2 and 3 receptors mediate a long range repulsion that specifies the lateral positions of axons running parallel to the midline (Guthrie, 1999). Furthermore, it appears that Robo is expressed at high levels on axons that do not cross the midline and that its expression is upregulated on the commissural axons upon crossing the midline (Kidd et al., 1999), consistent with its role as a repellent

The vertebrates also express three forms of Slit, Slit1, Slit2 and Slit3, respectively. Similar to *Drosophila*, the vertebrate Slit binds to Robo and regulates repulsive responses. In addition, the Slit pathway has been shown to play a pivotal role in the neuron cell body migration (Dirks, 2001; Wong et al., 2002; Wu et al., 1999).

ii. N-Cadherin: Adhesion and Growth Cone Navigation

The navigation of growth cones to their precise targets requires precise coordination between adhesive interactions and directional information from attractive and repulsive cues. Adhesion provides the growth cone with the traction necessary for movement, while the guidance cues signal directions (Goda, 2002; Steketee and Tosney, 2002). Additionally, adhesion allows follower growth cones to selectively identify the pathway laid out by pioneer axons and the appropriate axon fascicles. Though substantial evidence has been accumulated regarding axonal projection and cell adhesion individually, their interactive roles in the context of growth cone navigation remain elusive.

One adhesion protein family, the cadherins, represents a prominent adhesion mechanism important for axon pathfinding. In particular, the N-cadherins form transient but stable interactions important for growth cone navigation (Ranscht, 2000). In N-cadherin mutant flies, neuronal projection defects are apparent in all classes of photoreceptor axons (Lee et al., 2001).

Physically, N-cadherin has been linked to the actin cytoskeleton through members of the catenin family (Rhee et al., 2002). The β catenin for instance interacts with N-cadherin and α catenin in turn links actin to the N-cadherin/β catenin. In addition, the GTPases Rac, Rho and Cdc-42, which are important mediators of growth cone navigation, have been implicated in regulating the N-cadherin-catenin complexes (Rhee et al., 2002). The finding that the Robo pathway interacts with N-cadherin through Abl kinase further

highlights the importance of the coordination between cell adhesion and directional cues during growth cone pathfinding.

IV. Intrinsic Factors Linked to Growth Cone Cytoskeleton Restructuring

i. Guidance Signals propagated by GTPases

Although significant progress has been made toward identifying and characterizing extracellular guidance cues involved in growth cone pathfinding, much less is known about the linkage between these guidance cues and the reorganization of the cytoskeletal network. One regulator linking the guidance receptor with the cytoskeleton is the Rho family of GTPases (Luo et al., 2000).

GTPases bind to and hydrolyze guanosine nucleotides, resulting in the exchange of GDP for GTP and a structural change exposing effector-binding domains. Cycling between a GTP-bound and a GDP-bound conformation allows these GTPase molecules to function as intracellular switches (see Figure 1.3).

There are three types of proteins involved: Guanosine Nucleotide Exchange Factors (GEFs), GTPase Activating Proteins (GAPs), and Guanosine Dissociation Inhibitors (GDIs). GEFs facilitate the signaling pathway by promoting the conversion from the inactive GDP form to the active GTP state, while GAPs switch the pathway off by increasing the rate of the GTP hydrolysis. GDIs facilitate this process by inhibiting GDP-GTPase dissociation and keeping it in the inactive conformation (Luo et al.,2000).

GTPases Cdc42 and Rac1 have been implicated in regulating the formation of the growth cone filopodia and lamellipodia, respectively (Aspenström, 1999; Small et al., 2002), while the activation of GTPase RhoA leads to growth cone collapsing (Dickson, 2001). Thus these GTPases mediate both attractive and repulsive responses (Patel and Van Vactor, 2002). Furthermore, the effectors for these GTPases have been shown to regulate cytoskeletal dynamics. For example, Cdc42 is a co-activator of protein N-WASP that is involved in regulating cytoskeletal actin polymerization (Rohatgi et al., 1999). Given the worm UNC-115 has been shown to interact with Rac GTPases, it is intriguing that UNC-115 may act as a downstream component of an attractive guidance cue (Struckhoff and Lundquist, 2003).

ii. Trio as a GEF Regulating Axon Guidance

The Trio family of Guanine-nucleotide-Exchange-Factors (GEFs) has been identified for its importance in regulating the Rho family of GTPases during axon projection (Bateman and Van Vactor, 2001). A *Drosophila* Trio (*dtrio*) has been characterized and like the human and worm homologs, it has two GEF domains (Steven et al., 1998; Lin et al., 2000; Luo, 2000). Functionally, it appears that the first GEF domain interacts with Rac to convert it to an active form and to promote the formation of lamellipodia.

Expression patterns and phenotypic analyses have suggested for *dtrio* a role in the CNS development. Mutations in *dtrio* affect both the CNS and photoreceptor axon projections, where growth cones stall or miss their targets

with inappropriate fasciculation (Bateman and Van Vactor, 2001). Furthermore, axons from a subset of the CNS neurons undergoes defasciculation prematurely (Awasaki et. al., 2000; Bateman et. al., 2000). Similar phenotypes have also been observed in mutants of the worm Trio homolog UNC-73 (Bateman and Van Vactor, 2001; Steven et al., 1998)

Genetic interaction studies in *Drosophila* indicate that the non-receptor tyrosine kinase Abl is a downstream component of the *dtrio* pathway (Bateman and Van Vactor, 2001; Lanier and Gertler, 2000). In homozygous *abl* mutants, the CNS axons have similar pathfinding defects as *dtrio* mutants (Liebl et. al., 2000), including the thinning of commissures and longitudinal fascicles. In addition, double mutants heterozygous for *dtrio* and homozygous for *abl* have an exacerbated *abl* mutant phenotype (Liebl et. al., 2000). Conversely, when *abl* was mutated heterozygously in homozygous *dtrio* background, exacerbation of the *trio* phenotype has also been observed albeit at a lesser degree (Liebl et. al., 2000). The most severe phenotype was seen in homozygous *abl/trio* double mutants where commissures were missing and longitudinal axons disrupted (Liebl et. al., 2000).

Interestingly, genetic analysis in worms has shown that *unc-73*, *rac1* and *unc-115* may act in the same pathway during growth cone navigation (Gitai et al., 2003; Struckhoff and Lundquist, 2003), raising the possibility that UNC-115 is a guidance mediator regulating the cytoskeletal reorganization during growth cone navigation.

ii. Binding Proteins Involved in Remodeling the Actin Network

The ultimate goal of guidance cues is to elicit directional movement by restructuring the actin filament network of the growth cone (Dickson and Senti, 2002; Tessier-Lavigne and Goodman, 1996). Actin filaments elongate or contract by adding or removing actin subunits from either the barbed or the pointed ends, respectively (Figure 1.4). While elongation can occur at either end, polymerization is predominantly at the barbed end (Cooper et al., 2000).

There are three types of actin binding proteins, recognizing respectively barbed ends, pointed ends and filament sides. Two mechanisms are involved in regulating actin polymerization via the actin-binding proteins that recognize filament ends. One is capping of ends, preventing the addition and removal of actin subunits to the filament ends (Hug et al., 1995). The other mechanism termed nucleation involves formation of new filaments through promoting polymerization of actin monomers (Borisy et al., 2000). In lamellipodia, nucleation and capping of barbed ends result in free pointed ends leading to actin filament growth. Filament growth occurs through funneling, which is the recycling of actin subunits added to the remaining barbed ends (Borisy et al., 2000). Funneling in filopodia is the result of creating more pointed ends through severing followed by capping of barbed ends (Borisy et al., 2000). The pace for subunit dissociation is under the regulation of side binding proteins, which can either decrease or increase the rate of actin subunit removal (Cooper et al., 2000).

a. Barbed End Binding Protein - Villin

When actin subunits polymerize at the cell periphery during locomotion, the extension is via the newly generated free barbed ends (Cooper et al., 2000). One important controlling mechanism is the binding of capping proteins to the barbed ends, which in turn stops filament growth. Specifically, the capping proteins cap almost all barbed ends and filament growth only occurs at free barbed ends. As a result, loss of the capping proteins affects cell motility. For instance, in *Listeria*, a model system used in studying cell mobility and actin cytoskeleton, motility is reliant upon capping proteins (David et al. 1998; Loisel et al. 1999).

Villin is a multifunctional member of the Gelsolin protein family, with different domains specific to its different activities. There is a Gelsolin-like core domain functioning in capping and severing actin barbed ends (Friederich et al., 1999). The Villin headpiece domain is capable of bundling actin filaments both *in vitro* and *in vivo* (Friederich et al., 1999). Fibroblast cells, when ectopically expressing *villin*, are covered with microvilli containing bundled actin (Friederich et al., 1999).

In cells transfected with a villin variant lacking the headpiece domain, actin bundling is absent as a result of the inability of villin to bind actin. Although bundling has been observed in *in vitro* transfection experiments as well as in *Drosophila* oocytes, it is unclear whether bundling is Villin's main function (Cant et al., 2000). In *villin* knock-out mice, a mutant bundling phenotype has yet to be identified. The reason for a lack of phenotype may

be the result of a redundancy of bundling proteins (Cooper and Schafer, 2000).

In addition, actin bundling appears to be normal in intestinal epithelial cells lacking Villin, further highlighting the existence of redundancy and the difficulty elucidating actin bundling as the main function of Villin (Marks et al., 1998). In contrast, Villin deficient mice lack actin fragmentation, suggesting an aberration in the severing pathway (Ferrary et al., 1999). It is possible that the main function of Villin is severing barbed ends of actin filaments.

b. Pointed End Binding Proteins – Arp2/3 Complex

A pointed end protein such as Arp2/3 binds to the pointed ends and promotes the formation of actin filaments (Borisy et al. 2000). The Arp2/3 complex consists of at least seven protein subunits. The Arp2 and Arp3 subunits bind to actin filaments, while Arp 2/3 is present in areas of actin polymerization and at the leading edge of the lamellipodia (Takenawa and Miki, 2001). When the actin is in the presence of the Arp2/3 complex, a branching filament network is formed (Mullins, 1998), similar to that created in the cortex of migrating cells (Cooper et. al., 2000).

Signaling proteins that induce actin polymerization exert their functions through stimulating Arp 2/3 function. For example, the protein N-WASP upon co-operative activation by Cdc42 and phosphatidylinositol 4,5 bisphospate (PIP_2) directly activates Arp2/3's ability to polymerize actin filaments (Takenawa and Miki, 2001). Furthermore, N-WASP binds to Arp 2/3 directly as a strong activator (Takenawa and Miki, 2001). This provides a pathway

that regulates actin dynamics to elicit cellular movement (Rohatgi, 1999; Prehoda et al., 2000).

c. Side binding proteins – ADF/Cofilin

The actin depolymerizing factor (ADF)/Cofilin family consists of actin side binding proteins that function to destabilize filaments, a critical step during filament treadmilling. Treadmilling is the process of maintaining filament length through actin subunit removal from the pointed end and addition to the barbed end (Borisy, 2000). When ADF/Cofilin bind to actin filaments, a conformational change occurs that weakens subunit interactions, making filament severing more likely (Hayden et al., 1993; Theriot, 1997; Cooper et al., 2000). In addition, depolymerization may occur at a greater speed through releasing pointed end proteins as a result of filament conformational change. Destabilization occurs through severing filaments, resulting in more free pointed ends and an increased rate of depolymerization (Okada, et al., 1999; Cooper et al., 2000).

V. UNC-115 Orthologs

i. C. elegans *UNC-115*

The *C. elegans unc-115* gene was first identified in a genetic screen for an uncoordinated phenotype and subsequent analysis revealed multiple alleles with pathfinding defects in various subclasses of neurons (Lundquist et al., 1998). Two isoforms are generated through five prime end alternative splicing of the *unc-115* gene, encoding two proteins of 639 and 470 amino acids in length, respectively. Three LIM functional domains have been

identified in the longer form, while the shorter version has one and a half such domains. Functionally, the LIM domains are motifs engaged in protein-protein interactions (Bach, 2000). In addition, UNC115 also has a villin headpiece domain (VHD), a potential binding site for actin filaments (Struckhoff and Lundquist, 2003). Finally, these proteins carry the UNC-115, abLIM, dematin (UAD) domain with unknown functions.

The upstream signals that regulate *unc-115* are not well characterized. Recently, UNC-115 has been implicated in the Netrin guidance pathway either upstream or in a parallel pathway of the Netrin receptor UNC-40 (Gitai et al., 2003), raising the possibility that UNC-5 may function as a linkage between the Netrin guidance cues and the cytoskeleton. In addition, Ced-10 and Rac1 of the Rac GTPase family regulating growth cone guidance have been demonstrated to be functionally linked to UNC-115 in the same pathway or a parallel one (Gitai et al., 2003; Struckhoff and Lundquist, 2003).

ii. Vertebrate AbLIM

The first vertebrate UNC-115 ortholog identified is the actin binding LIM protein (AbLIM). Three alternatively spliced isoforms have been uncovered, abLIM-l, abLIM-m and abLIM-s according to size (Roof et al., 1997), which encode three proteins of 778, 701 and 545 amino acids in length. Like the worm UNC-115, each AbLIM protein has a VHD co-localized with actin filaments (Roof et al., 1997). Furthermore, these isoforms contain the UAD domain and a different number of amino terminal LIM domains (Roof et al., 1997).

Functionally, a dominant negative abLIM phenotype in the chick visual system shows crossovers of retinal ganglion cell (RGC) axon projections, wide gaps between axon bundles, and thicker bundling of the axons indicative of defasciculation defects (Erkman et al., 2000). Currently, the upstream signal regulating abLIM remains unclear, though a transcription factor Brn 3.2 that functions in axon pathfinding has been linked with abLIM expression (Erkman et al., 2000) .

VI. *Drosophila* as A Model for Axon Pathfinding

The fruit fly *Drosophila melanogaster* has long been a powerful genetic model. The amenability to molecular and cellular techniques has further extended the fly model to a wider range of issues including those related to the nervous system. With the completion of the *Drosophila* genome sequences, the system offers a unique model to probe *in vivo* functions of a variety of genes. Moreover, mounting evidence has firmly established the conservation of many core biological mechanisms and results obtained from the fruit flies will be highly informative for understanding more complex systems including humans.

i. Axon Pathfinding in the Visual System

a. Anatomy of the Visual System

Adult *Drosophila* compound eyes are composed of a hexagonal array of 750-800 discrete units called ommatidia, with females having approximately fifty more ommatidia than males (Wolff et al., 1997). One ommatidium contains eight photoreceptor neurons and eleven accessory

cells. The eight photoreceptor cells (R cells) are referred to as R1-8 with R1-6 forming a ring around R7 and R8 (Wolff et al., 1997). While the R1-6 cells extend the depth of the ommatidium, the central photoreceptor cells R7 and R8 lay stacked one above the other with R7 extending proximally 2/3 and R8 distally 1/3 of the depth of the ommatidium (Wolff et al., 1993).

During visual system development, R cells send axons in bundles traveling through the optic stalk and terminating at the visual processing center in the brain, the optic lobe (Wolff et al., 1997). The optic lobe consists of three ganglion layers, namely, lamina, medulla and lobula. They serve as specific targets for incoming photoreceptor neurons, with axons from R1-6 forming synapses in the lamina and R7-8 axons terminating at the medulla (Senti et al., 2000).

b. Visual System Development

The *Drosophila* compound eye is formed from the eye-antennal imaginal disc, a sac of epithelial cells (Wolff et al., 1997; Dickson, 1993). Eye development commences during the 3rd instar larval stage as a wave of precise pattern formation, coupled with cell differentiation in a posterior to anterior direction (Dickson and Hafen, 1993; Wolff et al., 1997; Treisman and Heberlein, 1998; Lee and Treisman, 2001). The leading edge of pattern formation is defined as the morphogenetic furrow, which sweeps anteriorly, leaving photoreceptor clusters behind in different stages of maturity.

The formation of each individual ommatidium follows a defined order of differentiation, where a photoreceptor core is formed first with the accessory

cells added afterward to generate an ommatidium (Wolff et al., 1997). Specifically, the R8 cell is the first to be specified, followed by the recruitment of other R cells in pairs, R2/5, R3/4 and R1/6. Finally, the R7 is added to the cluster to complete the photoreceptor neuron assembly (Zipursky et al., 1984; Clandinin and Zipursky, 2002).

Synchronized with the progress of the ommatidium development, the optic lobe develops under the partial signaling from the incoming retinal axons (Salecker et al., 1998; Zhen and Kunes, 1998; Huang and Kunes, 1996) giving rise to the three proliferating zones, the outer proliferation center (OPC), the lamina precursor cells (LPC) and the inner proliferation center (IPC) (Kunes et al., 1993; Kaphingst and Kunes, 1994; Wolff et al., 1997).

The retinal axon projection is a highly organized process driven partially by the positional information on the optic lobe (Kunes et al., 1993; Salecker et al., 1998). These axons traverse long distances, bypass other possible targets and terminate at their specific sites in the brain. The stereotypic projection pattern has offered a powerful model to study axon pathfinding. Indeed significant progress has been made in identifying genes critical for retinal axon navigation (Hing et al., 1999; Newsome et al., 2000; Dearborn et al., 2002).

However, it remains poorly understood how guidance cues are received and interpreted in reference to the reorganization of the cytoskeleton network leading to the navigation decision by growth cones. The retinal axon pathfinding during *Drosophila* visual system development provides one

opportunity to examine molecular mechanisms associated with growth cone projection.

ii. Axon Projection in the CNS

a. Anatomy of the Midline

The *Drosophila* embryonic ventral midline constitutes another site where axonal navigation is a major developmental stage. As shown in figure 1.7, neural axons project ipsilaterally and contralaterally, forming lateral and commissural bundles in the characteristic ladder-like appearance. Each repetitive unit defines a neuromere that contains longitudinal projections, anterior and posterior commissures, segmental (SN) and intersegmental (ISN) neuronal projections (Kaprielian et al., 2000).

b. Development of the Midline Projections

Most neurons of the CNS are interneurons which have long projections that cross the midline in a commissure and extend anterior or posterior during development (Kaprielian et al., 2001). Prior to crossing the midline, they exhibit no affinity for the longitudinal tracts, but upon reaching the contra-lateral side they join a longitudinal bundle (Kaprielian et al., 2000). The formation of the posterior and anterior commissures takes place between 8-10 hours of embryo development, coinciding with stage 12 of embryonic development that is subdivided into three stages based on segmentation, namely, 12/5, 12/3 and 12/0 (Goodman and Doe, 1993). The first growth cones that pioneer the posterior commissures occur at stage 12/5 and as these growth cones grow directly toward the midline, they make a short

anterior projection and then navigate toward the midline (Kaprielian et al., 2000). Once the axons reach the midline they contact and fasciculate with the contra-lateral projection to form the posterior commissure.

At stage 12/3, the anterior commissure is pioneered (Goodman and Doe, 1993) and in contrast to the posterior commissure, the anterior commissures project straight across the midline. As the anterior commissures project, they meet with the contralateral projecting and the posterior commissures (Hummel et al., 1999). By the end of stage 12/0, the anterior and posterior commissures separate (Goodman and Doe, 1993). It is thought that the separation of the two commissural bundles is induced by a subset of midline glia cell migration (Hummel et al., 1999). Ultimately, the growth cones of the posterior and anterior axons navigate anteriorly or posteriorly into one of the longitudinal fascicles(Kaprielian et al., 2000).

There are many subsets of longitudinal axon projections. As depicted in figure 1.7, a subset of longitudinal axons express Fas II, a marker for three bundles on each side of the midline: the inner MP1 bundles, the FN3 medial bundle, lateral bundle (Goodman and Doe, 1993). The longitudinal axon bundles are formed between 9 and 11 hours of development. Only the developmental pathways of the MP1 and MP2 projections have been well characterized (Kaprielian et al., 2000). Both the MP1 and MP2 projections are pioneered by the pCC growth cone. At 9 hours pCC extends anteriorly to pioneer the MP2 pathway (Goodman and Doe, 1993). Ultimately, the MP2 growth cones fasciculate to the pCC pioneer and follow its path. The MP1

growth cones extend laterally in a posterior direction forming the medial pathway. Finally the projections result in the generation of two MP1 and MP2 pathways that are separate pathways in neuromeres and fused between segments (Goodman and Doe, 1993).

c. Motorneuron Projections

There are 34 motor neurons that exit the CNS through intersegemental and segmental nerve roots (Goodman and Doe, 1993). The motorneuron project stereotypically (Landgraf et al., 1997). The ISN root projects on both sides near the boundary between adjacent neuromeres. SN roots project on both sides approximately in the middle of the neuromere. The ISN is pioneered by the aCC neuron (Goodman and Doe, 1993). Segment boundary cell, a glial cell located adjacent to the first developing longitudinal pathway, direct the formation of the ISN root (Landgraf et al., 1997). When the segment boundary cell is ablated the ISN does not form. The ISN and SN motor axons come together just outside of the CNS at the exit junction (Landgraf et al., 1997). These motor axons selectively separate into five major branches that project to different body wall muscles (Landgraf et al., 1997).

Though significant knowledge has been accumulated lately related to the mechanisms regulating nervous system formation, substantial gaps remain in areas such as how guidance cues are processed molecularly by the growing axons during navigation. One candidate gene, *unc-115/abLIM*, offers a unique opportunity to narrow some of the gaps. This gene encodes a

conserved cellular protein implicated in the axonal pathfinding in both worms and vertebrates (Erkman et al., 2000; Roof et al., 1997). What remains elusive is how this gene regulates axonal navigation and interacts with other guidance mechanisms.

To this end, I chose to use the *Drosophila* model to explore the molecular mechanisms associated with the fly homolog *dunc-115* pathway and given the cross species conservation, it is within expectation that results from the fruit fly model will be informative for understanding other more complex systems including humans.

Chapter 2. Materials and Methods

I. DNA Sequencing

i. Growing Clones

The cDNA clones were grown on 25 μg/ml chloramphenicol plates overnight at 37°C. Single colonies were picked and cultured overnight in 3 ml of NZCYM (Sigma) liquid media containing 12.5 μg/ml of chloramphenicol (Sigma) at 37°C with constant shaking.

ii. Plasmid DNA Isolation

Plasmid DNA was isolated using a mini-prep kit (Qiagen) and several modifications, outlined below, were made to the kit protocol to increase plasmid yield. The cells were pelleted from culture by centrifuging in 1.5 ml tubes at 12,500 rpm for two minutes and the supernatant was removed. The cells were resuspended in 250 μl of P1 Buffer and incubated at room temperature for five minutes. Cells were lysed, by adding 250 μl of P2 Lysis Buffer and incubated at room temperature for five minutes. The lysis buffer was neutralized by adding 350 μl of N3 solution and put on ice for ten minutes. Samples were centrifuged for fifteen minutes at 12,500 rpm and the supernatants were applied to spin columns and centrifuged for one minute at 5,000 rpm. The flow-through was reapplied two more times to the column, centrifuging after each application for one minute. The flow-through was discarded after the final application. The columns were then transferred to clean 1.5 ml tubes and the plasmid DNA was eluted from the columns with 10mM Tris-HCL pH 9.0. DNA elution was conducted by adding 50 μl 10 mM Tris-HCL pH 9.0 to column, incubating at room temperature for one minute,

and centrifuged at 6,000 rpm. The elution was repeated three more times and after the final elution, the samples were centrifuged at 12,000 rpm for one minute. The DNA concentration and purity was determined by OD260 and OD280 spectrophotometric readings.

iii. Determination of the Insert Size

Since the inserts of the *dunc-115* clones were directionally cloned with *EcoRI* and *Xho I* at each end respectively (see Chapter 3 for details), the insert size was determined by cutting the plamids with 5 U/μl *EcoRI* and *Xho I* and 1X NEB reaction buffer #2 (New England Bio Lab). The digestion products were analyzed on a 1% agarose gel.

iv. Initial Sequencing of Plasmid DNA

Initial sequencing of the cDNA insert was conducted by the thermocycle sequencing method using a Sequenase Kit (USB). The protocol included in the kit was used and the parameters optimized. Initially, termination mixes for each nucleotide was prepared on ice. Each termination mix consisted of 2 μl of nucleotide master mix and 0.5 μl of either [α ^{33}P] labeled ddGTP, ddCTP, ddATP or ddCTP (AP Biotech), thawed to room temperature per reaction. Next the reaction mix was separately prepared and consisted of 2 μl of reaction buffer, 2.5 pmol of T7 or PM001 primers (Sigma, Table 2.2), 150 ng of plasmid DNA, 8 U of Thermosequenase, and ddH_2O was added to a final volume of 20 μl. Aliquots of 4.5 μl of reaction mix was added to the G, A, T, C, termination tubes. The thermocycler and sample was preheated at 95°C for two minutes and the optimized sequence cycling

program was set: 95°C 30 seconds, 55°C 30 seconds, 75°C for 2 minutes per round of cycling for a total of 40 cycles. The reaction was stopped with 4μl of stop solution (USB) and pulse centrifuged.

Sequenced samples were analyzed on polyacrylamide gels. A single gel was prepared by adding 21 g of Urea (Fisher Scientific), 5 ml 10X TBE, 7.5 ml Sequal Gel Mix (Fisher Scientific), and ddH_2O to a final volume of 50 ml. To polymerize the gels, 500 μl of 10% ammonium persulfate and 60μl of TEMED were added. The gels were allowed to polymerize for 1.5 hours. To run the gel, 800 ml and 400 ml of 1X TBE was added to the top and bottom chambers respectively. Sequencing gels were pre-run for 50 minutes. Sequencing reactions were boiled at 95°C for 5 minutes and 4 μl were loaded on the gel. Gels were run for 20 minutes then 100 ml of 5M KOAc was added to the bottom chamber. The sequencing gels were run for 2.5-3.0 hours, were put in fixative (10% methanol and 5% acetic acid) for 30 minutes and transferred to filter paper. The gels were dried under vacuum for 30 mins and exposed to film overnight.

Sequences were read and analyzed by searching the BDGP and NCBI databases. Three plasmid clones that appeared to encode three different forms of *dunc-115* were sequenced in full by a commercial source (GeneWiz).

v. Complete Insert Sequencing and Assembly

The plasmid cDNAs chosen for full-length sequencing were AT12805, SD01878, and SD03267 (Table 2.1). These cDNAs originated from different cDNA libraries the AT and SD libraries, which were generated from the

Drosophila adult testis and Schneider cell line, respectively. The inserts of the AT library were directionally cloned into the pOTB7 vector (see figure 2.1) where the 5' end and 3' end of the insert were subcloned using EcoRI and *XhoI* sites, respectively. The inserts of the SD library were directionally cloned using the pOT2 vector (see figure 2.2). This vector has the EcoRI and XhoI sites in an opposite orientation in comparison to the pOTB7 vector. The 5' end of the insert was subcloned using the *XhoI* cloning site while the 3' end used the *EcoRI* site.

Isolated plasmid DNA from each clone was submitted to GeneWIZ (North Brunswick, NJ) at a concentration of 1 μg with the necessary primers for various rounds of sequencing. Sequencing of the insert was considered complete when the sequence from opposing sides overlapped with high fidelity. It took approximately 4 rounds of sequencing per clone to sequence the full insert. After each round, the sequence was analyzed using BLAST searching and compared to the predicted sequence using GCG. The initial round of sequence was obtained using vector primers T7 and PM001 at a concentration of 7.5 pmol. The 5' end of inserts in the pOT2 vector can be sequenced with T7 primer while the 3' end can be obtained using the PM001 primer. In contrast the 5' end of the insert in the pOTB7 vector can be sequenced using PM001 and the 3' end can be obtained using the T7 primer.

Once sequence was obtained from the initial sequencing, primers were designed to reliable sequence and sent out for synthesis (SIGMA) (Table 2.2). Once the primers were received they were resuspended in 500 μl of

ddH_2O and diluted to a working concentration of 2.5 pmol/μl. Samples were sent to GeneWIZ containing 7.5 pmol of primers and 1 ug of plasmid DNA for the next round of sequencing. Once the data was received from GeneWIZ, the sequence was analyzed and the new primers were generated and samples were sent to GeneWIZ for the next sequencing round. Approximately two more rounds were sent for sequencing using primers designed to reliable sequence and synthesized by SIGMA. Table 2.2 contains is a list of primers generated for sequencing.

Sequences were assembled using the GCG program and full-length cDNAs defined as the longest open reading frame (ORF) containing both the initiation and stop codons.

II. Bioinformatic Analysis of Sequences

i. Comparison of cDNA Sequences

To determine the differences between the three *dunc-115* clones, cDNA sequences were aligned to each other using the GCG program. Additionally, intron and exon boundaries were determined by comparing the assembled cDNA sequences and the genomic sequences obtained from the genome database (AE003683).

ii. Conceptual Translation of Full-length cDNAs

The three full-length sequences were conceptually translated into all six reading frames by the GCG and the longest reading frame identified.

The three different amino acid sequences were compared with each other using the Cluster W (www.ch.embnet.org/index.html) and the GCG

programs. Protein sequence comparison was also conducted among homologs from different species.

iii. Identification of Functional Domains

The conceptually translated isoforms were submitted to a Pfam (http://pfam.wustl.edu) and Motif (http://motif.stanford.edu) search to identify functional domains. To identify the presence of the UAD domain that is characteristic of this family of proteins (see text for details), the consensus sequence from vertebrates and *C.elegans* was obtained and gapped in GCG (Lundquist et al., 1998). Once the domains were identified the percentage identity was analyzed with AbLIM and UNC-115 orthologs using the GCG pile-up command and Cluster W.

III. Expression Analysis of *dunc-115*

i. Northern Blot Analysis

a. Isolation of Total RNA

Embryonic RNA was used to conduct the Northern blot analysis. Embryos were collected overnight for approximately 18 hours on grape juice plates with yeast paste. The embryos were collected and washed with autoclaved 0.1% DEPC treated water to remove the yeast. Approximately, 100 μl of embryos were soaked in 0.1% DEPC treated water for 5 minutes and then homogenized with 1 ml of UltraSpec solution (BIOTECX). The homogenate was placed at 4°C for five minutes and the RNA was extracted by adding 200 μl of chloroform with vigorous shaing for 15 seconds. The solution was then placed on ice at 4°C for 5 minutes and centrifuged at

12,000 g at 4°C for 15 minutes. The aqueous phase was collected and RNA was precipitated with an equal volume of isopropanol at 4°C for 10 minutes. Samples were pelleted by centrifuging at 4°C for 10 minutes at 12,000 g, washed two times with 1 ml of 75% EtOH, and resuspended in 100 μl of 0.1% DEPC treated water. Concentration and purity was measured by taking OD_{260} and OD_{280} readings.

b. Transferring RNA to Membrane

RNA transfer to membranes was conducted using the Northern Max Kit (Ambion) with modifications. RNA samples were run on a 1% denaturing agarose gel and transferred to a positively charged membrane. The denaturing gel was prepared by melting 0.5 g of agarose in 45 ml of DEPC water, followed by the addition of 5 ml of 10X denaturing buffer, generating a gel approximately 0.6 cm in thickness.

The embryonic RNA samples were loaded in two lanes, one lane to probe for *dunc-115* and the other for the tubulin positive control. Another lane was designated for the RNA marker. Prior to loading, 30 μg of RNA per lane was mixed with three volumes of formaldehyde load dye (Ambion) and denatured by heating at 80°C for 10 minutes. The RNA ladder was prepared the same way using a concentration of 2μg (Sigma). Samples were placed on ice and loaded on the gel. Gels were run in 1X MOPS Buffer (Ambion) at approximately 5 V/cm, until the loading dye reached the bottom of the gel. The wells and lanes containing the ladder were trimmed off. The gel section containing the ladder was stained with ethidium bromide for 20 minutes.

Subsequently, the slab containing the ladder was wrapped in Saran wrap, placed overnight at 4°C and de-stained the next day in 1X MOPS buffer.

The section of the gel containing the embryonic RNA was prepared for transferring by rinsing the gel with DEPC treated water followed by soaking for 20 minutes in 0.01N NaOH/3M NaCl. A downward transferring orientation was used to transfer the total RNA to a Bright Star plus positively charged nylon membrane (Ambion). The bottom of the gel was placed on the transfer stack directly contacting the top of the membrane and the orientation of the gel was marked by notching the gel and outlining the edge to the membrane. Transfer was done overnight for approximately 18 hours using 20X SSC as the transfer buffer. The membrane was washed at room temperature for 5 minutes in 20X SSC, air dried and baked under vacuum for two hours. So that both lanes can be probed differently, the two lanes were separated using sterile scissors.

c. Generation of Probes

The *dunc-115* and beta-1 tubulin specific probes were generated and labeled with ^{32}P-dCTP. Probes were generated using Polymerase Chain Reaction (PCR). The PCR reaction mix was set up using 2.5 µl of 10 X PCR Buffer (Fisher Scientific), 1.5 µl of $MgCl_2$ (Fisher Scientific), 5 µl of (1.25mM dATP, dTTP, dGTP and 0.12mM of dCTP) dNTP mix, 8 µl of ^{32}P CTP, 0.8 ug of each primer, 0.8 µl of Taq polymerase (Fisher Scientific), 150 ng of DNA template and water to a final volume of 25 µl per reaction.

For generating the *dunc-115* specific probe the plasmid DNA from clone SD01878 was used as a template with sequencing primers MG5P1 and MG3P1 (see Table 2.2). To generate the tubulin probe primers TUBUP2 and TUBDN2 (SIGMA) were used with plasmid DNA from a clone containing a beta-1 tubulin specific insert (Table 2.2). The probes were boiled for 10 minutes at 95°C and placed on ice.

d. Hybridization

Membranes were place in separate sealable bags with 7 ml of ULTRAhyb hybridization solution (Ambion) to submerse membranes for one hour at 42°C. The probes were boiled and injected into bags at a concentration of 1ul of probe/ 1ml of hybridization solution. The blots were allowed to hybridize overnight at 42°C with rocking.

To remove residual unhybridized probe, membranes were washed one time for 30 minutes at room temperature with 1XSSC, 0.1% SDS. Following the initial wash, membranes were washed three times for 30 minutes each at 68°C with 0.5 SSC, 0.1% SDS. Membranes were dried on filter paper for a few minutes, sealed in a bag and exposed to film for 18 hours at -75°C.

ii. In situ hybridization

a. Collection of Embryos

Canton S adult flies about five days old were placed in a collecting chamber with a grape juice plate covered with yeast paste for 1 to 2 days to condition the flies (Ashburner, 1989). Grape juice plates were made by boiling together 220 ml water, 170.4 ml grape juice (Welch's), 9 g of fly agar

(SIGMA), 23.2 g glucose (SIGMA), 11.6 g sucrose, and 7.2 g of yeast 500+vitamin (Fisher). After the mixture is cooled 4.5 ml of Acid Mix A and 8.8 ml of 1.25N NaOH was added. The mixture is then poured into small Petri plates that fit the collecting chamber and allowed to harden. Water and yeast are mixed to form a paste that is spread on the plates.

The flies are left in the collecting chamber and embryos are collected on the plates overnight, approximately 18 hours. The plates are exchanged and embryos are removed from the overnight plate by using a small paint brush and washing with water into a collecting basket.

b. Fixation of Embryos

To remove the yeast paste embryos were washed well with water and dechorionated with 50% bleach for 3 minutes. The embryos were then rinsed thoroughly with water and placed into a glass test tube containing a mix of 1 ml of heptane and 1 ml of 4% paraformaldehyde with the fixative phase at the bottom. The vial was agitated for 1 hour at room temperature, followed by the removal of the aqueous phase leaving behind the heptane and embryos. To remove the vitelline membrane, 1 ml of methanol was added to the tube and shaken vigorously for 1 minute. Those embryos that have been devitellinized sank to the bottom and were washed three times with methanol following the removal the liquid. The embryos were stored in methanol at -20°C until use.

c. Generation of RNA Probes

RNA probes for the sense and anti-sense strands of *dunc-115* were generated and DIG-labled using plasmid DNA from clone SD01878. Initially,

5 μg of plasmid DNA was linearized by digesting with 100U of *XhoI* and *BstXI* to respectively generate sense and anti-sense probes. After digestion, DNA was purified by extracting with phenol:chloroform and back extracting with Tris-HCl pH 9.0. The linearized DNA was precipitated with 1/10 the volume NaOAc pH 5.2 and 2.5 the volume of 100% EtOH. The precipitate was pelleted by centrifugation at 12,500 rpm for one hour and washed with 70% EtOH. The pellet was resuspended in nuclease free water.

To generate the DIG labeled probe, the plasmid insert was transcribed *in vitro*. The sense strand was generated using T7 RNA polymerase, while the anti-sense strand was generated using Sp6 RNA polymerase enzyme mix. *In vitro* transcription T7 and Sp6 reactions were set up containing 2 μl 10X Reaction Buffer (Ambion), 2 μl10X DIG labeling mix (Roche), 1μg of linearized plasmid DNA, and 2 μl Enzyme Mix (Ambion). The reaction mix was incubated for 4 hours at 37°C. DNA was removed by treating with 2U of RNase-free DNaseI (Ambion) for 15 minutes at 37°C. The transcription reaction was stopped and RNA precipitated by adding 30 μl nuclease-free water and 25 μl LiCl precipitation solution (Ambion). Samples were stored overnight at -75°C. RNA was pelleted by centrifugation at 12,500 rpm for 30 minutes, washed with 70% EtOH and resuspended in 50 μl of nuclease free water. Probe was analyzed on a 1% Agarose gel.

d. Hybridization

Prior to prehybridization and hybridization, embryos were rehydrated by washing two times for 5 minutes each and one time for 30 minutes with

PBT. The embryos were digested with 10 μg/ml proteinase K in PBS/Tween 20 for 10 minutes with gentle inversion and washed two times with 2 mg/ml glycine in PBS/Tween 20. Embryos were post-fixed with 4% paraformaldehyde in PBS for 20 minutes. The embryos were washed five times in PBS/Tween 20 for 20 minutes per wash, rinsed with 50%PBS/50% hybridization solution, and pre-hybridized for one hour at 55°C in 100% hybridization mix. The probes were prepared by adding 1 ng of probe to 100 ul of hybridization mix and heated at 85°C for 10 minutes. The probe solution was added to the embryos and hybridized overnight at 55°C.

e. Detection of Probes

Embryos were washed at the hybridization temperature for 20 minutes per wash in 1 ml of hybridization mix, 1ml in 1:1 hybridization solution/PBS-Tween, and five times in 1m of PBS/Tween 20. To detect the DIG labeled probe, hybridized embryos were incubated in a 1:5000 dilution of α-DIG-alkaline phosphatase antibody in PBS/Tween 20 for 1 hour at room temperature with rotating. Residual antibody was removed by washing four times with PBS/Tween 20 at room temperature with rotating. The embryos were washed three times at 5 minutes per wash with 1 ml of levamisole solution. To the final application of levamisole, 4.5 μl of NBT and 3.5 μl of X-phosphate were added.

The samples were kept in dark during the reaction checking periodically to monitor the dark blue staining. Proper development took approximately 10 minutes and the reaction was stopped by washing three

times with PBS/Tween 20. To mount and analyze expression pattern, embryos were put through a glycerol series of 25%, 50% and 80% and spread out on slide with the cover slip raised.

III. Stocks

i. Maintenance of Stocks

Stocks in current use were kept at 25°C in plastic vials or bottles with fly food at the bottom. Fly food is prepared by boiling Jazz Mix (Fisher Scientific), Caltech medium as a supplement and water. The food is cooled and the anti-mycotic agent Nipagen is added. The mixture is poured into vials or bottles and allowed to harden. Yeast is sprinkled on the surface prior to putting flies in the vessels.

ii. Fly Strains

The following stocks have been used:

Canton S, *y[1]; P{y[+mDint2] w[Br.E.Br]=SUPor-P}CG9489[KG03651]ry506, y[1]w[1]; Sb[1]/TM6B, Tb[+], TM3, ry[RK] Sb[1] Ser[1]/TM6B, Tb[1], y[1] w[*]; CyO, H{w[=mC]=Pdelta 2-3} HoP2.1/Bc[1] Egfr[E1]* and *yw*

iii Excision Strains

Excision strains were generated through crossing with a transposase strain and then generating a stock. See figure 2.3 for crossing scheme.

IV. Phenotypic Analysis of the Visual System

i. DAB Immunohistochemistry

a. Dissection and Fixation of the Third Instar Visual System

Third instar larvae were collected into a pool of PBT (1X PBS, 0.3% triton) under the dissecting microscope and the eye/brain complex dissected (Kunes et al, 1993). Freshly dissected visual systems were transferred to fresh PBT and then transferred to fresh 4% paraformaldehyde and fixed overnight at 4°C.

b. Staining of the Photoreceptor Neurons

Fixed visual systems were washed three times with 1 ml of PBT and blocked in 300 μl of BSTN (PBT with 10% goat serum) for 1 hour at room temperature prior to antibody incubation, followed by overnight incubation at 4°C with the photoreceptor neuron specific mouse monoclonal antibody 24B10 (Developmental Studies Hybridoma Bank) diluted 1:3 in BSTN. Residual antibody was removed by washing four times with PBT at room temperature for 15 minutes per wash and the samples blocked with BSTN for 1 hour at room temperature (He, 2000).

The visual systems were then incubated with horseradish peroxidase (HRP) conjugated goat anti-mouse polyclonal secondary antibody at a dilution of 1:200 at room temperature for 2 hours followed by washing three times in PBT at room temperature for 15 minutes per wash to remove unbound antibody molecules.

The DAB visualization was performed by adding to the samples a mix of 0.5 mg/ml of DAB and 3% hydrogen peroxide while monitoring the colorization of the solution. When the proper intensity was achieved in approximately 3 minutes, the reaction was stopped by washing three times

with PBT. Prior to mounting on slides, the brains were put through a glycerol series of 25%, 50% and 75% concentrations.

ii. Fluorescent Immunohistochemistry

a. Specimen Preparation

Third instar larvae were removed from the side of the stock bottles and placed in a pool of PBT under the dissecting microscope for dissection. Freshly dissected visual systems were transferred to PBT and fixed overnight at 4°C in 4% paraformaldehyde.

b. Visualization of the Retinal Axon Projections

To remove the fixative the visual system tissue was washed three times with PBT at room temperature for 15 minutes per wash. The brains were blocked in BSTN for one hour. Tissue was incubated overnight at 4°C in the pan-neural marker, FITC conjugated goat anti-horse radish peroxidase (Cappel) diluted 1:10 in BSTN. Residual antibody was removed by washing four times with PBT at room temperature for 15 minutes per wash. Prior to mounting, visual systems were put through a 25% and 50% glycerol series. Tissues were put in 70% glycerol containing an anti-quenching agent (p-Phenylenediamine di-hydrochloride) for mounting.

iii. BrdU Analysis

a. Preparing the Visual System

Third instar larvae of Cantons S and *dunc-115* strains were removed from the side of the stock bottles and placed in a pool of Graces medium (Gibco) under the dissecting microscope. Using surgical tweezers the larvae

are grabbed by the posterior end and the anterior end. To dissect the brain the two ends are pulled and tissue surrounding the visual system removed. The dissected visual systems were transferred to a vial containing 30 μg/ml of 5'-bromo-2'-deoxyuridine (BrdU) in Graces medium and incubated for one hour at room temperature. The BrdU treated visual systems was transferred to fresh 4% paraformaldehyde and fixed overnight at 4°C.

b. Examining the BrdU Incorporation

To remove fixative, the tissue was washed three times in PBT at room temperature for 15 minutes each wash. The tissues were depurinated with 2N HCl in PBT for 40 minutes at room temperature. To remove the acid solution completely, the tissue was washed three times in PBT. Visual systems were blocked with BSTN for one hour and incubated overnight at 4°C with 1:50 diluted mouse anti-BrdU (Becton Dickinson) in BSTN. Residual antibody was removed by washing four times in PBT at room temperature for 15 minutes per wash. The tissue was blocked with BSTN for one hour. Following blocking, the tissue was incubated overnight at 4°C in 1:25 diluted Cy3-conjugated goat anti-mouse secondary antibody (Jackson ImmunoResearch Laboratories, Inc.) and 1:10 FITC-conjugated goat anti-horse radish peroxidase (Cappel) in BSTN. The tissue was washed four times at room temperature with PBT for 15 minutes per wash. Prior to mounting the samples were subjected to a 25% and 50% glycerol series. Tissues were put in 70% glycerol containing the anti-quenching agent for mounting.

iv. Microscopy

a. Mounting the Specimens

Stained specimens were mounted to slides in either a lateral perspective or a coronal orientation depending on the staining (see text). All samples were mounted in 70-75% glycerol.

b. Confocal Microscopy

A Nikon PCM-2000 confocal microscope equipped with dual HeNe-Argon lasers was used to analyze the samples. The scope has a FITC filter set, power stage control and the Simple-32 computer software.

V. Phenotypic analysis of the midline

i. Sample preparation

a. Collection of Embryos

Canton S and *dunc-115* adults were put into a collecting chamber for conditioning, and eggs were collected overnight for approximately 18 hours on grape juice plates covered with yeast paste. Embryos were washed with water into a nylon basket and rinsed well to remove residual yeast.

b. Fixation of Embryos

To remove the chorion the embryos were soaked in 50% bleach for three minutes. The embryos were fixed on a 4% paraformaldehyde and heptane interface for one hour. The vitelline membrane was removed by methanol. Embryos were washed and stored in methanol at -75°C. Prior to staining the embryos were re-hydrated by washing two times for five minutes

and one time for 30 minutes with PBT. Embryos were blocked for 1 hour with BSTN prior to staining.

ii. Immunohistochemistry

a. Fluorescent Staining

To investigate the midline several antibodies were used. Embryos were incubated overnight at 4°C with 1:3 mouse anti-BP102 in BSTN. To remove residual antibody, the embryos were washed four times for 15 minutes each in PBT. Subsequently, embryos were blocked in BSTN for one hour and incubated overnight at 4°C with 1:25 diluted Cy3-conjugated goat anti-mouse secondary antibody (Jackson ImmunoResearch Laboratories, Inc.). Embryos were washed four times in PBT for 15 minutes each wash. Prior to mounting embryos were put through a 25% and 50% glycerol series. The embryos were put in 70% glycerol plus an anti-quenching agent for mounting.

Double staining was conducted by incubating embryos overnight at 4°C with 1:3 mouse anti-FasII in BSTN. Embryos were washed four times for 15 minutes each in PBT and blocked in BSTN for one hour. Subsequently, embryos were incubated at 4°C in 1:25 diluted Cy3-conjugated goat anti-mouse secondary antibody (Jackson ImmunoResearch Laboratories, Inc.) and 1:10 FITC-conjugated goat anti-horse radish peroxidase (Cappel) in BSTN. Embryos were washed four times for 15 minutes each and put through a 25% and 50% glycerol series. The embryos were put in 70% glycerol containing an anti-quenching agent for mounting.

b. Mounting for Microscopy

Embryos were spread out on a slide in the 70% glycerol containing the anti-quenching agent and a cover slip was mounted with the cover slip raised using two cover slips to form a "bridge" configuration to preserve the morphology. Also by rolling the cover slip, embryos were positioned to the desired orientation.

Chapter 3. Identification of the *dunc-115* Gene

I. Identification of *dunc-115*

One major task in elucidating mechanisms governing axon pathfinding is to identify genes essential for the wiring of the three dimensional neural circuitry (Tessier-Lavigne and Goodman, 1996). The completion of the *Drosophila* genome project has provided a unique opportunity to probe the *in vivo* functions of genes essential for the CNS development (Meyers et al., 2000). One candidate is the *unc-115* gene in *C. elegans* that plays a pivotal role in organizing the nervous system development (Lundquist et al., 1998). Moreover, ample evidence has shown that *unc-115* may function as an important downstream component of the Netrin guidance cue (Gitai et al., 2003). By applying the molecular, cellular and genetic tools available to the fly system, it should be possible to obtain further understanding of the *unc-115* pathway. To this end, I set out to first identify the *Drosophila unc-115* homolog, *dunc-115*.

i. Bioinformatics

To identify *dunc-115*, I took a reverse genetic approach where I first searched the fly sequence database and then obtained the cDNA clones encoding *dunc-115*. Specifically, I used the *C. elegans* cDNA sequence (GenBank#AF068867) to query the fly database. One annotated sequence corresponding to the *dunc-115m* I later sequenced (see text below) was obtained (CG9489), along with several EST sequences. They formed the starting point of my search for the fly *dunc-115* homolog.

ii. Identifying Possible Full Length dunc-115 *cDNA Clones*

Expressed Sequence Tags (ESTs) are 5' or 3' sequences from cDNA clones that are approximately 300 to 500 bp in length. From the BLAST analysis, fifteen ESTs were identified (Table 2.1) and using the GCG program, their sequences were matched to the *dunc-115* predicted sequence. Clones were identified as potentially containing full length *dunc-115* inserts if the EST sequences extended beyond the presumptive initiation codon or the stop codon. Together, six such clones were identified and obtained from the distributor Research Genetics (Table 2.1).

After in house sequencing three of the six clones were identified as being unique. The three cDNA clones, SD01878 (3.3 Kb), SD03267 (2.7 Kb) and AT12805 (2.4 Kb), were sequenced and proven to contain full-length *dunc-115* sequences (see Figure 3.1). The sizes of the full-length cDNAs vary and each was named according to their size; *dunc-115l* (SD01878), *dunc-115m* (SD03267), and *dunc-115s* (AT12805), respectively.

All full-length sequences have unique 5' sequences and *dunc-115l* has an exclusive 3' sequence. Each cDNA contains an ORF with the ATG start codon preceded by an in-frame stop codon. As shown in figure 3.1, both *dunc-115m* and *dunc-115s* contain the stop codon TAA, while *dunc-115l* has TAG. All cDNAs contain a polyadenylation signal and a poly A tail. Based on the sequences, *dunc-115* has been mapped to 85E6 of chromosome 3R.

Comparison with the Berkeley Drosophila Genome Project (BDGP) genomic sequences has made possible the identification of intron and exon boundaries. Thus the *dunc-115* gene spans some 10.7 Kb and contains

eleven exons that appear to be alternatively spliced to generate the three isoforms identified (Figure 3.1).

II. Functional Domains

Upon conceptual translation, three amino acid sequences of varied lengths were identified. Similar to the cDNA clones, Dunc-115l is the longest containing 806 amino acids (aa), while Dunc-115m has 769 aa and Dunc-115s the shortest with 766 aa. Figure 3.2 shows the comparison of the three amino acid sequences.

Using bioinformatics tools, I examined the domain structure of these isoforms and their cross-species comparison with other orthologs (Figure 3.3, Garcia and He, 2003). Similar to vertebrate abLIM-I, the Dunc115 protein contains four N-terminal LIM functional domains. Unlike other orthologs, the three isoforms of Dunc-115 do not have any varying LIM domains. Given LIM domains are important for mediating protein-protein interactions (Bach, 2000), it is forseeble that Dunc-115 isoforms may use LIM domains to interact with other proteins. In addition, all three isoforms contain the UAD domain (**UNC-115, AbLIM, Dematin**), though its function remains elusive (Lundquist et al., 1998).

Dunc-115l and m share a 19 aa domain that is not found in Dunc-115s (Figure 3.2). I was unable to identify any functional association for this stretch of 19 aa (YIRSRTPSFNGSLYSSSRK) through database searching. While all Dunc-115 orthologs have a C-terminal villin head piece domain (VHD), only Dunc-115l possesses one such domain. Since the VHD domain has been

shown to interact and bundle with actin filaments (Friederich et al., 1999), it is tempting to envision that the Dunc-115 VHD domain may interact with the actin network in neurons.

To investigate the conservation during evolution, a cross-species protein comparison was carried out. As shown in table 3.1, the isoform Dunc-115l shows the highest level of identity at 44.8% with the vertebrate homolog, abLIM-l. This result is not surprising since similar to abLIM, Dunc-115l has four LIM domains, a UAD domain and a VHD domain. Dunc-115m and Dunc-115s show a higher percentage identity with the abLIM long form than with their respective medium and short forms. Once again this is linked to the fact that both Dunc-115m and Dunc-115s have four highly conserved LIM domains. Although Dunc-115m and s do not share the highest percentage identity with the respective medium and short isoforms of abLIM, the conservation of all three forms of Dunc-115 with the abLIM isoforms is striking considering the evolutionary distance between *Drosophila* and vertebrates.

In addition to the high percentage identity shared with abLIM, Dunc-115 shares a high percentage of identity with the long form of UNC-115. Figure 3.3 illustrates the conservation between the long forms of all three orthologs. The striking conservation shared by these proteins indicates a possible functional conservation as well.

The similarities between Dunc-115 isoforms and their orthologs were further examined between the functional domains. Table 3.2 shows the percentage identity between the LIM domains of Dunc-115l and abLIM-l. All

of the LIM domains of the Dunc-115 isoforms have the same amino acids. I numbered the most N-terminal LIM domain as #1 and the rest followed in numerical order (see Figure 3.4). There is a considerable conservation between the LIM domains of abLIM-I and Dunc-115, with percentage identities ranging from 56% to 65%. As shown in figure 3.5, LIM domains #4 of Dunc-115 and #3 of UNC-115 correspond to each other with a striking percentage identity of 69%.

Only Dunc-115I has a VHD domain and it has significant conservation with the VHD of abLIM and UNC-115. As shown in figure 3.5, the VHD domain of Dunc-115 has a percentage identity of 64% with the nematode and 58% with vertebrates.

III. Expression of *dunc-115*

i. Northern Blot

The tissue expression pattern of a gene is often an informative indicator for the possible functioning sites of the gene. To evaluate the *dunc-115* expression pattern, I conducted Northern blot and *in situ* hybridization analyses. As shown in figure 3.1, a *dunc-115* specific probe that spans a region common to all isoforms was used with total embryonic RNA in a Northern blot to identify expression of *dunc-115* as well as the presence of multiple isoforms. As shown in figure 3.6B, the Northern shows a diffused band ranging from 2.0 Kb to 3.5Kb, indicating the existence of multiple *dunc-115* messenger species. Furthermore, the sizes of our cDNAs fall with in the range of these mRNA species. Given other forms of orthologs in other

species, it remains possible that more *dunc-115* isoforms may yet be identified.

ii. In situ Hybridization

To further examine the tissue expression pattern of *dunc-115*, I carried out *in situ* hybridization using *dunc-115l* as a probe. The choice was based on the fact that *dunc-115l* should reveal all three isoforms given it is the longest.

The full-length *dunc-115* was used to generate anti-sense and sense probes to cross-react with all *dunc-115* isoforms. As shown in figure 3.6A, *dunc-115* messengers are expressed ubiquitously at the early embryonic stage 6, though maternal contribution cannot be ruled out. As the embryonic stage progresses, there is a localization of *dunc-115* messenger to the ventral and procephalic neurogenic region that can be seen in the stage 10 embryos (Figure 3.6A). Since the ventral midline is being constructed during this time, it is possible *dunc-115* may function during CNS development.

Indeed as embryogenesis progresses, a more intensified staining in the CNS and the region of the future visual system appears. In addition, there is an intense staining of *dunc-115* in the developing gut of the stage 12 embryos (see Figure 3.6A), indicating a possible involvement of *dunc-115* outside the nervous system.

IV. Conclusions

Three *Drosophila dunc-115* isoforms have been identified and they are likely to be the result of alternative splicing. The Northern blot shows the

existence of multiple *dunc-115* messengers and it remains possible that more *dunc-115* isoforms may exist.

Conceptual translation and bioinformatics analyses for functional domains of Dunc-115 have indicated a remarkable degree of conservation over the course of evolution. More importantly, it suggests that Dunc-115, like its counterparts in other species, may exert pivotal functions in the nervous system development, which will be directly examined in my future functional analysis.

Chapter 4. Phenotypic Analysis in the Visual System of a *dunc-115* Mutant

The structural conservation of Dunc-115 proteins across species implies a possible functional conservation as well. The high levels of expression in the nervous system are consistent with a role in the wiring of the CNS. To explore the involvement of Dunc-115 in the construction of the visual system and the midline in flies, I decided to search for a mutant strain.

I. The *dunc-115 P*-element Insertion Strain

To begin with, I searched the fly stock centers and located one P-element strain mutated at the *dunc-115* locus from the *P* element Screen Disruption Project (www.flypush.imgen.bcm.tmc.edu/pscreen). Using the GCG program, I compared the flanking sequences provided by the *P* element Screen Disruption Project to map the location of the *P* element to *dunc-115*. As diagramed in figure 3.1, the *P* element mapped to a location 260 bp from the 5' exon. These animals are homozygous viable and the third instar larva appear more svelte than wild type.

II. Retinal Axon Projections

To investigate whether the *dunc-115* mutant has an affect on photoreceptor axon projections, the visual system of the third instar larvae was stained with the photoreceptor neuron marker anti-24B10. Figure 4.1 shows the results from Canton S and *dunc-115* mutants. In wild-type brains, the photoreceptor neurons send their axons in a smooth bundle through the optic stalk and upon reaching the brain; they fan out evenly in a stereotopic fashion forming the crescent-shaped lamina plexis. As seen in Figure 4.1, *dunc-115* photoreceptor axons showed defective fasciculation as indicated by the large

gaps between the optic bundles (arrowheads). Furthermore, frequent crossovers were clearly visible (white arrow in Figure 4.1). Together, these data suggest that Dunc-115 proteins are involved in navigation decision making at choice points and proper defasciculation of retinal axons.

III. Lamina target region

The lamina is the target region for the R1-6 photoreceptor growth cones and to investigate the role of *dunc-115* in target selection, I stained brains with the pan-neural marker anti-HRP. In the wild-type brains, the R1-6 photoreceptor projections terminated in the target region termed the lamina plexis and as shown in Figure 4.2, the termini of the photoreceptor axons form the continuous crescent-shaped lamina plexis. In comparison, the *dunc-115* brains showed frequent gaps in the lamina plexis along with crossovers, indicating that the growth cones have difficulty reaching their proper targets. Upon excision of the *P* element the crossovers as well as gaps are no longer observed (Figure 4.3). Taken together, it appears that *dunc-115* plays a critical role in target recognition, possibly through regulating proper defasciculation.

IV. Cell division in *dunc-115* mutants

One possible scenario is that *dunc-115* may influence cell division and thus impact neural cell fate determination. To clarify this possibility, I carried out the BrdU incorporation analysis where only dividing cells would be labeled. In the wild type visual system, BrdU marks the three proliferation centers of the optic lobe, namely, the OPC, LPC and IPC (Figure 4.4), as well as demarcates the second mitotic wave in the eye disc. In comparison, the *dunc-115* optic lobes

have the same three proliferation centers being marked by BrdU, indicating a normal cell division in these animals. In addition, the *dunc-115* eye disc shows a similar cell division pattern as in the wild type.

V. Conclusion

Analysis of the *dunc-115* mutant strain has shown clear aberrant projections of the photoreceptor axons to optic lobe. In particular, defects are visible early within the retinal axon bundles traveling in the optic stalk as abnormal gaps and exacerbated into crossovers and larger gaps nearing the lamina target, highlighted by the frequent gaps within the lamina plexis. Collectively, it appears certain that *dunc-115* is a pivotal navigation regulator likely to exert its influence through impacting axonal defasciculation.

The cell division analysis confirms that *dunc-115* does not affect neural cell proliferation, making it unlikely that *dunc-115* may influence cell fate determination.

Chapter 5. Role of *dunc-115* at the Midline

The *Drosophila* ventral nerve cord or the midline offers another unique environment for examining axonal navigation. The well defined neuron classes should potentially generate fine details about the projection decision making of these neurons. I therefore extended my investigation to the midline to test the functional impact of *dunc-115*.

I. Axon Projections at the Midline

As shown in Figure 5.1, the BP102 marker specific for the CNS axons was used to stain the midline projections as well as intersegmental (ISN) and segmental (SN) neuron projections in the *dunc-115* mutant and wild type. Midline axon projections of wild type embryos show the characteristic ladder-like appearance that consists of the longitudinal as well as anterior and posterior commissural axons. The repetitive neuromeres are consistently spaced as seen from the lateral view. In addition, the SN neurons project off the neuromere, while ISN neurons project between the anterior and posterior commissures of adjacent neuromeres.

In *dunc-115* mutants, we see that the longitudinal bundles appear to be thicker, indicating an abnormal defasciculation. Indeed, the SN projections appear to have less intense staining and their projection is abnormal. As shown by the arrows in Figure 5.1, the SN axons project off at an abnormal angle of projection; these branching errors indicate that the axons do not project to their appropriate targets. Additionally the lateral view of the *dunc-115* ventral midline shows abnormal spacing of the neuromeres. The neuromeres of the mutants appear to be spaced closer together than that of the wild-type. Thus, it appears

that *dunc-115* plays a role in axonal defasciculation at the midline, similar to the visual system.

II. Fas II Expression and Longitudinal Axon Projections

To further examine the possible functional pathway that was affected by the mutation of *dunc-115*, I chose to explore the expression of the surface protein Fas II that marks the MP1, FN3 and lateral bundles and has been shown to influence their navigation decision at the choice points. To this end, I stained the midline with anti-Fas II antibody and in Figure 5.2, we see the three parallel Fas II staining bundles of the wild type longitudinal axons. The anti-HRP show commissural axons, all longitudinal bundles, SN and ISN projections.

In *dunc-115* mutants, we see an abnormal patterning of the Fas II staining longitudinal bundles. Specifically, the MP1 bundle abnormally defasciculates, producing four tracts and then fasciculates to form three tracts again (arrow in 5.2). In addition, there are breaks in the lateral bundle and thickened regions at the end of these breaks. These observations are consistent with the defasciculation defects seen in the BP102 stained ventral midline.

In addition to the defasciculation defects, the mutants exhibit abnormal crossing of the Fas II staining bundles indicating choice point decision errors (arrowhead in 5.2). The mutant exhibits defects in the SN projections consistent with those observed previously. The anti-HRP staining of mutants show commissural axons with thickness similar to wild type and we see thickening of the longitudinal bundles consistent with the observations seen in the BP102 stained samples. When both red and green channels are overlaid it is clear that

the thickening of the longitudinal bundles coincides with breaks in the lateral bundles as well as the defasciculation defects. Breaks also coincide with the region of SN projections. Additionally, these defects were not observed in wild type or the excision strains (Figure 5.3). These results indicate that *dunc-115* functions in choice point decisions as well as influencing defasciculation.

Over expression of Fas II causes axons to abnormally fasciculate with the inability to defasciculate. Since *dunc-115* and wild-type Fas II levels appear to be at the similar level, it is unlikely that *dunc-115* affects axonal navigation through influencing Fas II expression.

III. Conclusion

The embryonic ventral midline of *dunc-115* mutants exhibit thickened longitudinal bundling that is indicative of the inability of axons to defasciculate. Upon a more detailed analysis of the longitudinal bundles with double staining of anti-Fas II and anti-HRP, frequent breaks in the Fas II expressing bundles were observed. Moreover, the thickening of the longitudinal bundles coincides with formation of the breaks. Together, it seems clear that Dunc-115 proteins function as key mediators for axonal projection at the midline. Given the Fas II expression is not affected with mutation of *dunc-115*, we speculate that Dunc-115 functions independent of the Fas II pathway.

Chapter 6. Discussion

I. *dunc-115* is an Alternatively Spliced Gene with Multiple Isoforms

The availability of genome sequences from several species including fruit fly provides a unique opportunity to investigate gene functions of orthologs through reverse genetics. Indeed my initial goal was to identify and characterize the fly homolog of the *unc-115* gene that had been implicated in the axonal navigation in the worms (Lundquist et al., 1998). It was our expectation that using the well established fly system, it would be possible to gain further insights into the functional role of this gene in the nervous system.

I started my hunt for the fly homolog by searching the then newly established fly genome database and pulled out an annotated sequence and several EST clones. My initial sequence analysis revealed that these clones indeed encoded a *Drosophila unc-115* homolog and the completed sequences of three representative clones gave rise to three isoforms named *dunc-115l*, *m* and *s*, respectively. The three isoforms share most of their exons, suggesting a product of alternative splicing. Indeed Northern blotting has confirmed the existence of multiple mRNA species, consistent with this notion.

The proteins encoded by the three cDNAs, Dunc-115l, m and s, contain major structural similarities including the LIM domain and the UAD domain. Furthermore, Dunc-115 isoforms share extensive structural similarities with the worm and vertebrate orthologs. Dunc-115l in particular has the highest level of conservation with the vertebrate abLIM-I, where both

have four LIM domains and one VHD domain. While the VHD domain has been found in all vertebrate and worm homologs, it is absent in Dunc-115m and s, making Dunc-115m and s novel members of this extended family. It is plausible that other yet unidentified isoforms may exist.

II. Dunc-115l May Bind and Regulate the Growth cone Actin Network

Given that the VHD domain of UNC-115 has been shown to bind to actin filaments, it is highly possible that the VHD domain in Dunc-115l may also mediate interactions with the cytoskeleton. In addition, the LIM domains have been implicated in versatile protein-protein interactions (Bach, 2000), making it plausible that Dunc-115 may interact with other cellular proteins through the LIM domains.

The fact that both UNC-115 and Dunc-115 are involved in regulating axon navigation strongly indicates a functional connection between axonal pathfinding and the VHD mediated interaction with the actin fiber. It is our expectation that one mode of function for Dunc-115 is to influence growth cone projections through regulating the cytoskeletal network

III. *dunc-115* Regulates Navigation Decisions at Choice Points

The complete axon trajectory can be broken down into a series of segments, where a choice point marks the end of a segment and the beginning of another (Kaprielian et al., 2001). Thus decisions made by a growing axon at the choice points are critical for the entire axonal navigation. It appears that mutation of *dunc-115* results in errors at the choice points.

Photoreceptor axons project to the lamina in the brain in a stereotypic fashion where incoming axons innervate the lamina target in a directional movement from the posterior to the anterior, forming a typical crescent-shaped termination termed lamina plexis. In the visual system of *dunc-115* mutants, clear projection defects were visible where retinal axons appeared having navigation difficulty with the formation of folded axon bundles at the place of defasciculation prior to the lamina. In addition, retinal axons in these animals showed frequent crossovers accompanied by the formation of large gaps in the R1-6 target region, a clear indication of navigation errors and inappropriate defasciculation. Together, these data strongly indicate a role for *dunc-115* at the navigation choice points during retinal axon pathfinding.

Since Fas II has been implicated in regulating defasciculation at the choice points, I examined the midline axon projection in *dunc-115* mutants. The Fas II expressing axons exhibit three continuous tracts on either side of the wild type midline, while in *dunc-115* mutants, frequent breaks were seen with increased thickening at the branch points where segmental and intersegmental axons exit. In addition, the Fas II fascicules showed wavy appearance, consistent with a wiring abnormality. Furthermore, the segmental neurons exhibited branching errors with abnormal angles exiting the midline.

Taken together, it is clear that *dunc-115* plays a pivotal role in organizing axonal pathfinding in the midline and it does not appear *dunc-115* functions through influencing Fas II expression since the level of Fas II is comparable in both the wild type and the *dunc-115* mutant animals. We favor

a model where the Dunc-115 proteins interact with the cytoskeletal network, directly or indirectly, which in turn impacts growth cone navigation.

It is worth noting that similar phenotypes have been observed in the *C. elegans unc-115* mutants (Lundquist et al., 1998), where a subclass of neurons made erroneous navigation choices and formed abnormal fascicules. Thus *dunc-115* and *unc-115* appear to have conserved functions. Indeed the vertebrate homolog *abLIM* has also been implicated as causing axonal defasciculation defects in a dominant negative study.

IV. *dunc-115* May Regulate Axon Defasciculation Through Cytoskeleton Reorganization

The navigation of growth cones during the formation of axon trajectories requires a combination of adhesive interactions and guidance cues (Rhee et al., 2002), it remains poorly understood as how they influence each other. One study has shown the interaction of the guidance receptor Robo with the cell surface adhesion protein N-cadherin through Abelson kinase (Rhee et al., 2002), raising the possibility that *dunc-115* may play a role downstream guidance receptors to link with surface adhesion proteins.

The structure of Dunc-115l makes it a candidate for integrating the guidance pathways and the actin cytoskeleton reorganization. Similar to its orthologs, Dunc-115l has a highly conserved villin head piece domain (VHD). Given that the vertebrate abLIM VHD has been shown to co-localize and bind to F-actin and that mutated UNC-115 VHD domain fails to associate with F-actin, it is highly possible that Dunc-115l may interact directly with F-actin through its VHD domain to influence the cytoskeletal network.

Although Dunc-115m and Dunc-115s lack the VHD domain, they along with Dunc-115l may exert their functions by integrating of guidance cues and adhesion pathways through their LIM domains. Indeed the *C. elegans* homolog UNC-115 has been implicated as a possible downstream component of the Netrin receptor UNC-40 pathway and certain GTPases during axon projection (Gitai et al., 2003; Struckhoff and Lundquist, 2003). It is intriguing to directly examine the functional linkage between Dunc-115 and the Netrin guidance cues in *Drosophila*.

VI. Future Directions

i. Silencing dunc-115 through Heritable RNA Interference

Inducible RNA interference (RNAi) is the degradation of transcripts of a target gene by *in vivo* expression of an inverted repeat under the control of a UAS promoter, and a hairpin structure is generated upon induction of the inverted repeat with a Gal4 driver (Lam and Thummel,2000; Kennerdell and Carthew, 2001; Schmid et al., 2002). Since it has been repeatedly shown to be an effective way of silencing a target gene (Lum et al, 2003), it would be a plausible approach to selectively silencing different forms of *dunc-115* and hence shed light on their possible functional differences.

To test the effectiveness, I have started to generate a construct that will silence all three isoforms by targeting a shared sequence. Specifically, I have generated a construct using the pWIZ vector (Lee and Carthew, 2002) that is a *P* element vector with a 74 base pair spacer and a UAS site. If

proven effective, it will be possible to selectively silence *dunc-115l, dunc-115m,* and *dunc-115s.*

The availability of tissue-specific Gal4 drivers has made it easy to induce a tissue specific silencing of *dunc-115.* For example, the silencing can be induced in the eye disc only to probe the involvement of different isoforms of *dunc-115* in the visual system wiring. Given the available markers for different R cells, it is possible to examine whether *dunc-115* functions preferentially on certain types of retinal axons.

ii. Generation of Multiple Alleles

A more conventional alternative is to generate more *dunc-115* alleles through P-element local hopping (Liao et al., 2000; Tower et al., 1993; Zhang and Spradling, 1993). Specifically, the P-element can be mobilized and re-inserted into a new location with in the *dunc-115* locus, making it possible to generate isoform-specific mutants. The examination of the phenotype from these strains should shed light to the functional differences between isoforms.

Together, it is our expectation that we will gain further insights into the involvement of *dunc-115* in the nervous system construction.

Appendix A. Chapter Tables

Chapter 2 Tables

Chapter 3 Tables

EST Clones	cDNA Library	Vector
GM05872	Ovary	pOT2
GH13330	Adult head	pOT2
GH08475	Adult head	pOT2
GH13731	Adult head	pOT2
SD03267	**Schneider cells**	**pOT2**
SD01878	**Schneider cells**	**pOT2**
SD07509	Schneider cells	pOT2
LP11002	Larvae, pupae	pOT2
HL01353	Adult head	pOT2
AT12805	**Adult testes**	**pOTB7**
AT02731	Adult testes	pOTB7
AT08430	Adult testes	pOTB7
AT24641	Adult testes	pOTB7
AT11722	Adult testes	pOTB7

Table 2.1 EST clones screened for full length cDNAs
This table shows the fourteen clones analyzed for potential full length sequences. The clones are derived from different cDNA libraries made from different sources. The last column shows the different vectors that carry the inserts.

Primer names	Primer sequence
T7	5'-TAATACGACTCACTATAGGG-3'
PM001	5'-CGTTAGAACGCGGCTACAAT-3'
MG5P	5'-CACCGGCGGATTCTTCACA-3'
MG3P	5'-GGTAGGAATGTATGGCATTG-3'
MG-S	5'-GGTTGCTATCCTCGCATGC-3'
MG5P1	5'-GGCAAGGTGCTCCAAGCG-3'
MG3P1	5'-TCCGAGCGGATGGCGTCCAC-3'
TUBUP2	5'-CGGAAGCTTCTAGACCATGTCC-3'
TUBDN2	5'-CGGAAGCTTGGCGTGGGTCGCAG-3'

Table 2.2 Primers used in sequencing and generating probes.
This table shows the various primers used in sequencing full length cDNAs and generating probes for the Northern blot.

% Identity	Dunc-115l	Dunc-115m	Dunc-115s
abLIM-l	44.8%	39.9%	40.3%
abLIM-m	43.9%	39.1%	40.5%
abLIM-s	38.5%	31.1%	33.5%
UNC-115	42.4%	37.0%	36.3%

Table 3.1 Percentage identity between the three Dunc-115 isoforms and its homologues

Dunc-115l shows the most identity to abLIM-l and UNC-115, which corresponds to the presence of the LIM domains and a villin headpiece domain. Eventhough, Dunc-115m and Dunc-115s lack the same number of LIM domains and a villin headpiece domain as in abLIM-m, abLIM-s and UNC-115 they still share a significant percentage identity with abLIM-l.

LIM domains of abLIM-l	Dunc-115l LIM Domains			
	% Identity	#1	#2	#3	#4
	#1	56.1%	37.0%	35.7%	30.4%
	#2	28.6%	50.0%	37.1%	34.7%
	#3	28.6%	26.8%	64.9%	37.8%
	#4	44.6%	31.0%	63.0%	63.3%

Table 3.2 Percentage identity between LIM domains of Dunc-115l and abLIM-l

This table illustrates the percent identity between the four LIM domains of Dunc-115l and the corresponding domains of abLIM-l. There considerable identity between the four LIM domains.

Appendix B. Chapter Figures

Chapter 1

Chapter 2

Chapter 3

Chapter 4

Chapter 5

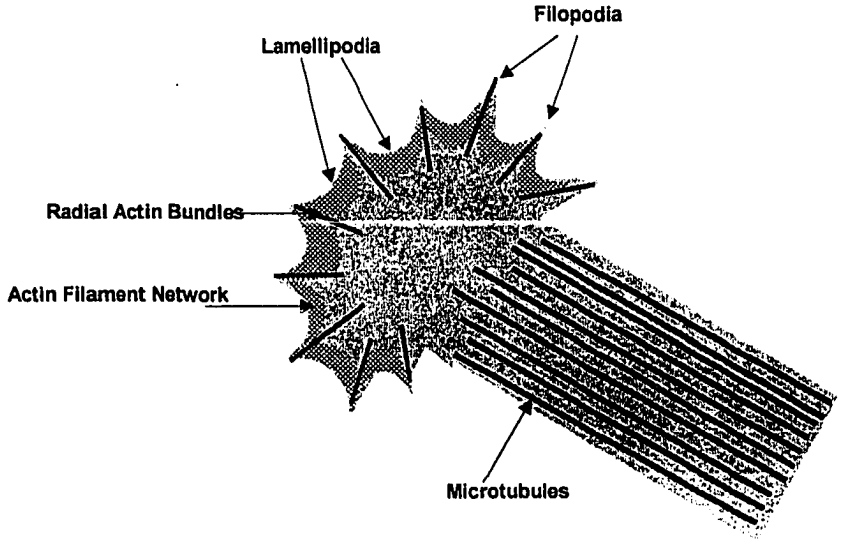

Figure 1.1 Growth cone morphology
The growth cone has web-like structures called lamellipodia. Underlying this structure is an actin network. The filopodia are spike-like structures that are supported by radial actin bundles.

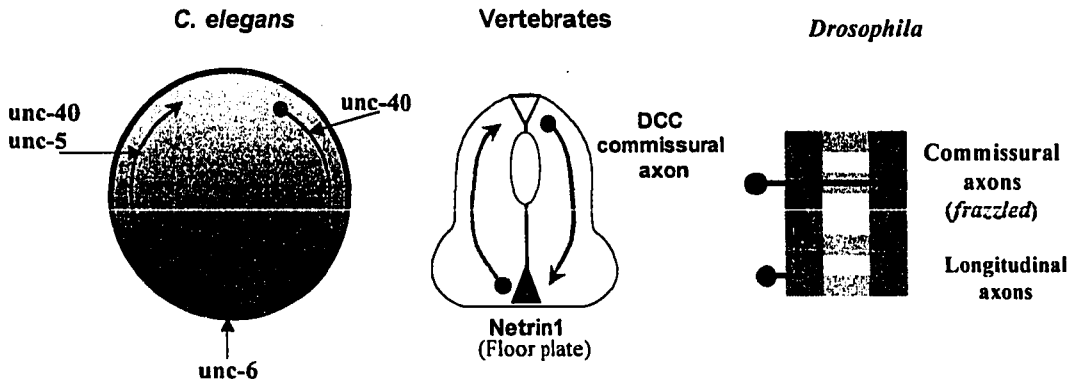

Figure 1.2 Netrin orthologs and their mechanism of action.

(A) Attraction of UNC-40 and repulsion of UNC-5/UNC-40 positive neurons in response to an UNC-6 gradient in C. elegans. (B) Commissural axons of the vertebrate spinal cord are attracted to the Netrin expressing floor plate. (C) The *Drosophila* ventral midline has a characteristic ladder-like shape made of midline crossing commissural axons and repelled longitudinal axons.

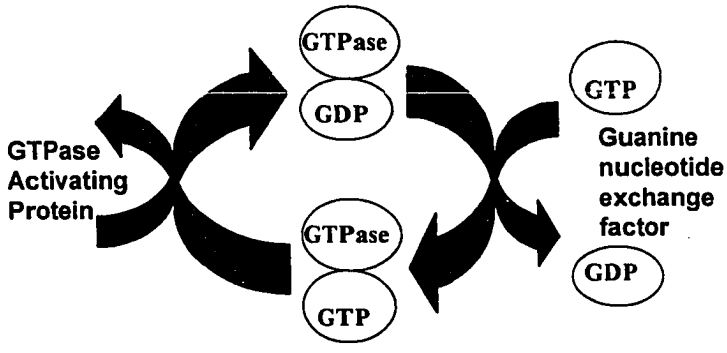

Figure 1.3 GTPase mode of action.
The GTPase cycles between a GTP and a GDP bound state. The exchange for GDP for GTP is facilitated by the guanine nucleotide exchange factor. The GTPase activating protein enhances GTP hydrolysis (adapted from Luo, 2000)

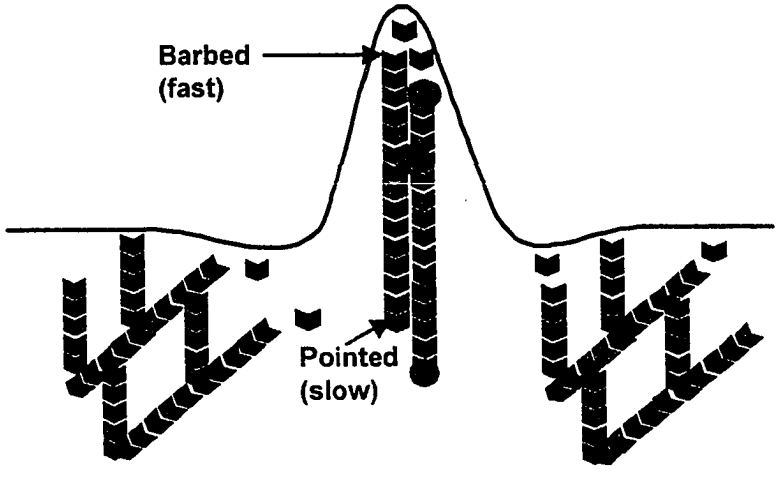

Figure 1.4 Actin remodeling in the growth cone
The addition of new subunits to actin filaments occurs at different rates. Assembly occurs at a more rapid rate at the barbed end when compared to the pointed end. Actin binding proteins regulate actin remodeling. These proteins can bind to the barbed end, pointed end or side of the filament.

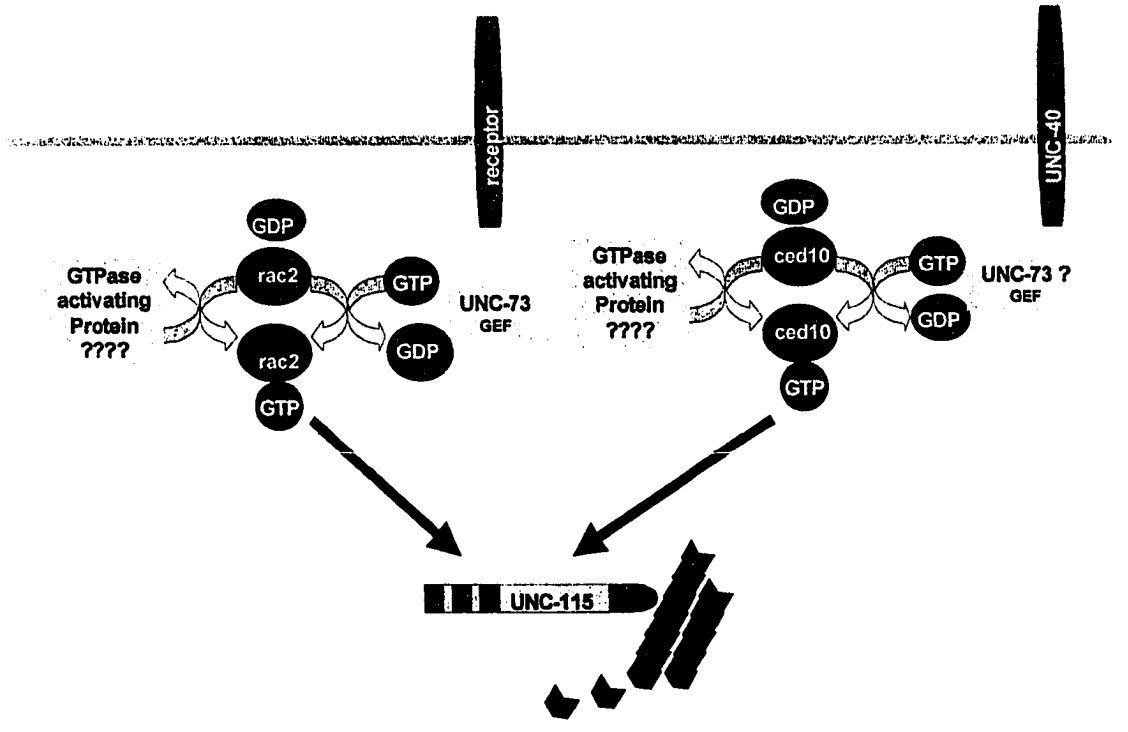

Figure 1.5 Proposed UNC-115 pathway
Based on recent genetic interaction studies in *C. elegans*, it appears that UNC-115 may act downstream of two pathways mediated by GTPases Rac2 and Ced10 as well as the guidance receptor DCC.

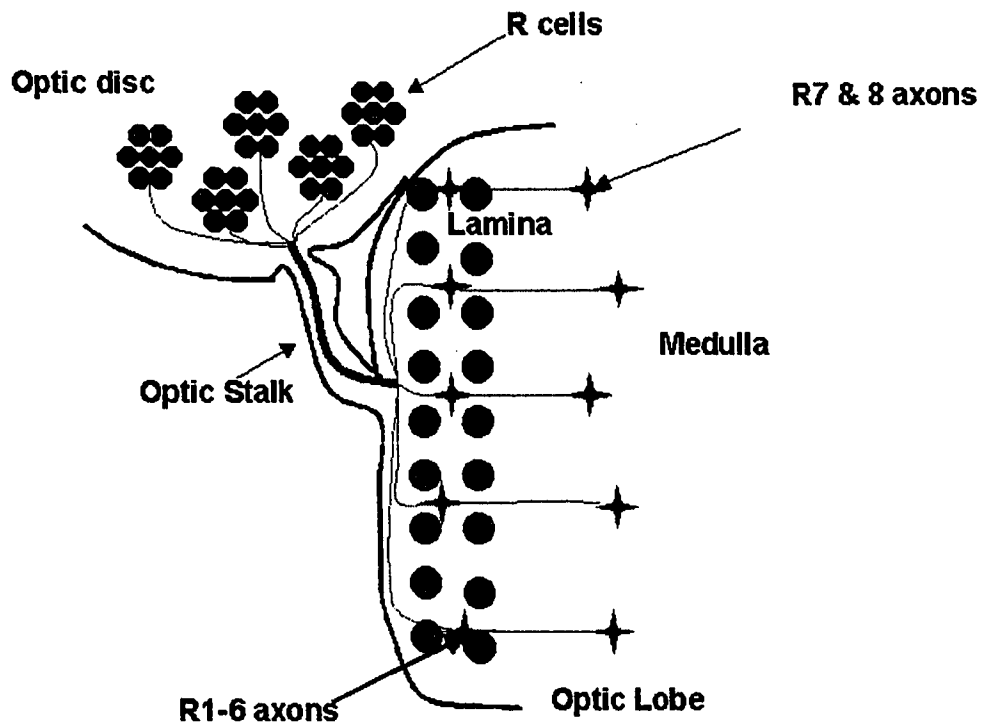

Figure 1.6 The visual system
The eight photoreceptor cells (R cells) project axons through the optic stalk. R cells 1-6 terminate in the lamina target region whereas R7 and 8 growth cones terminate in the medulla.

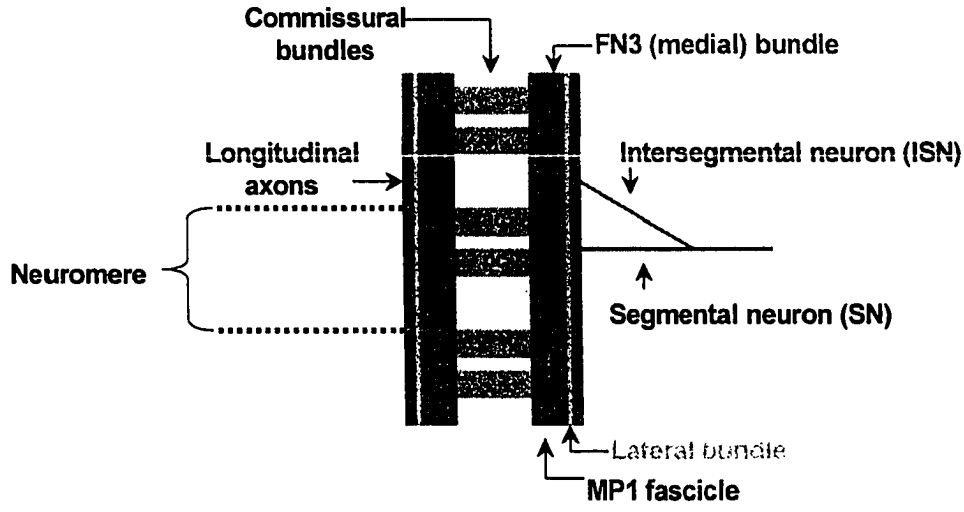

Figure 1.7 The ventral midline
The midline consists of longitudinal and commissural axon bundles. During development some cross the midline forming the anterior and posterior commissures (ac and pc). Some cross project laterally. These projections characterize the ladder-like appearance of the midline. The dotted line indicates a neuromere. Each neuromere has an ac, pc, intersegmental neuron (ISN) and segmental neuron (SN) projections. A subset of longitudinal axons the inner MP1 bundles, the FN3 medial bundle and lateral bundle express Fas II.

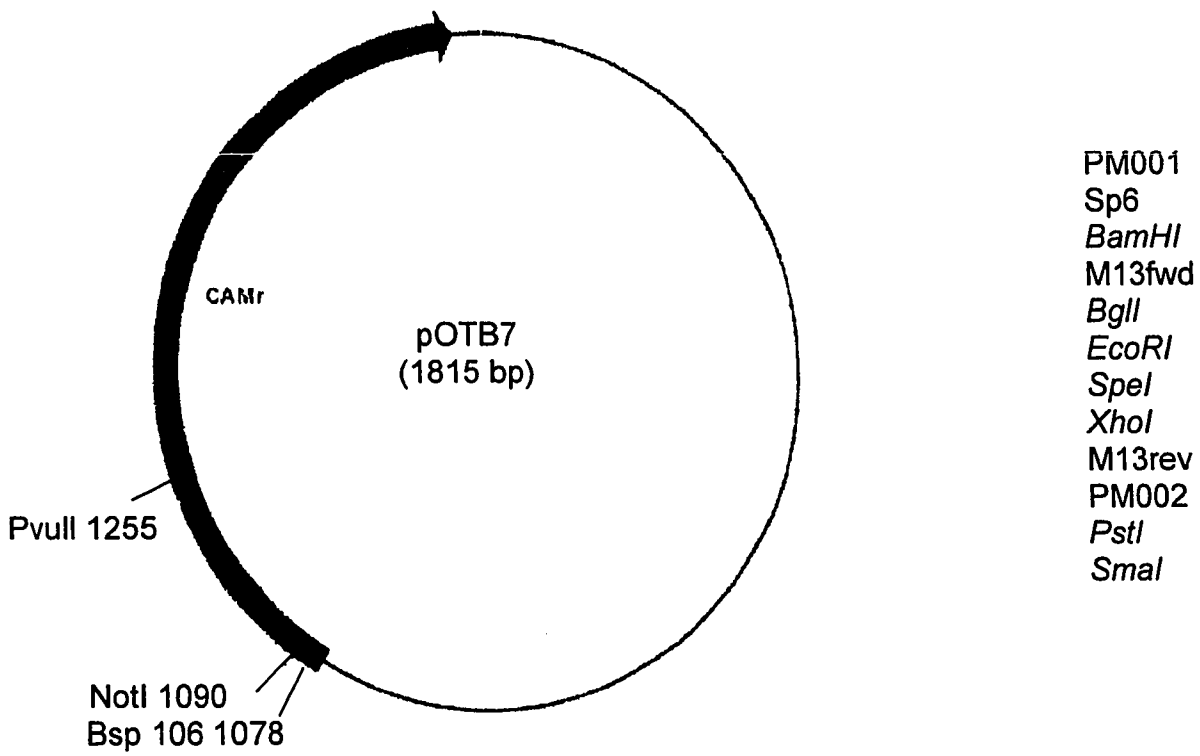

Figure 2.1 The pOTB7 vector. The pOTB7 vector was used to carry cDNA in the AT12805 sequenced clone. When compared to the pOT2 vector the insertion sites in this vector are reversed in relation to the sequencing sites. The cDNA is directionally inserted into *EcoRI* and *XhoI* sites. The 5' end of the cDNA sequence was obtained using PM001 and the 3' end was obtained using T7 sequencing primers

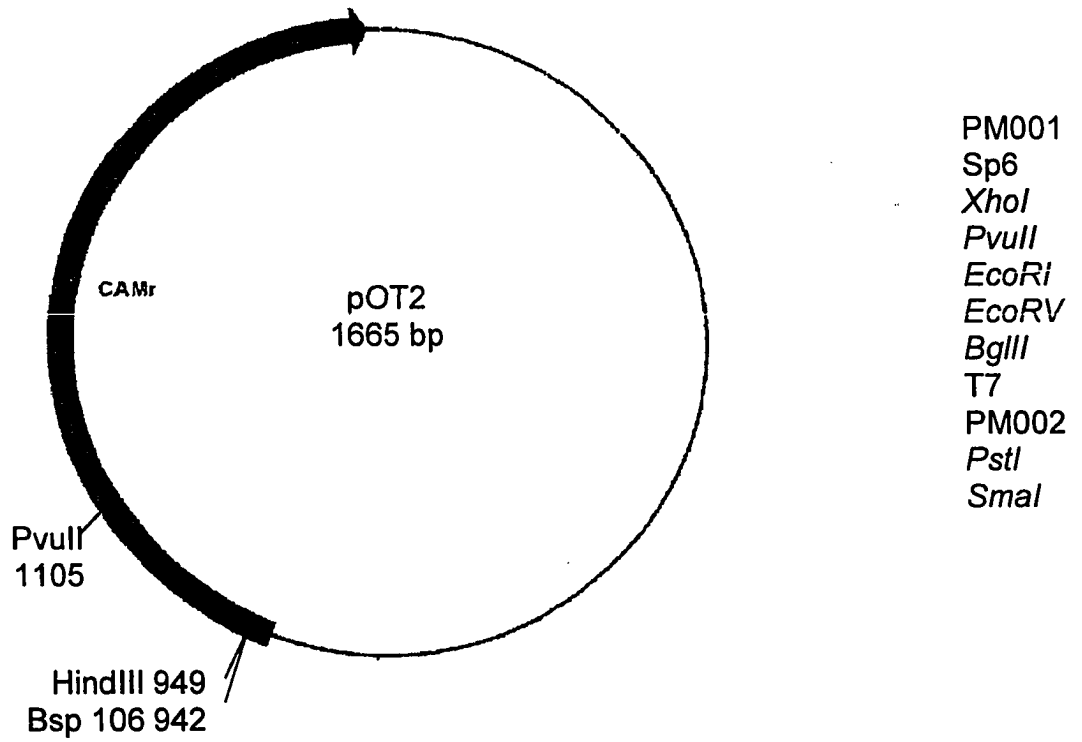

Figure 2.2 The pOT2 vector. The pOT2 vector was used to carry cDNA in SD01878 and SD03267 sequenced clones. The cDNA is directionally inserted into the 5' *EcoRI* and the 3' *XhoI* sites. The 5' end of the cDNA sequence was obtained using T7 and the 3'end was obtained using PM001 sequencing primers.

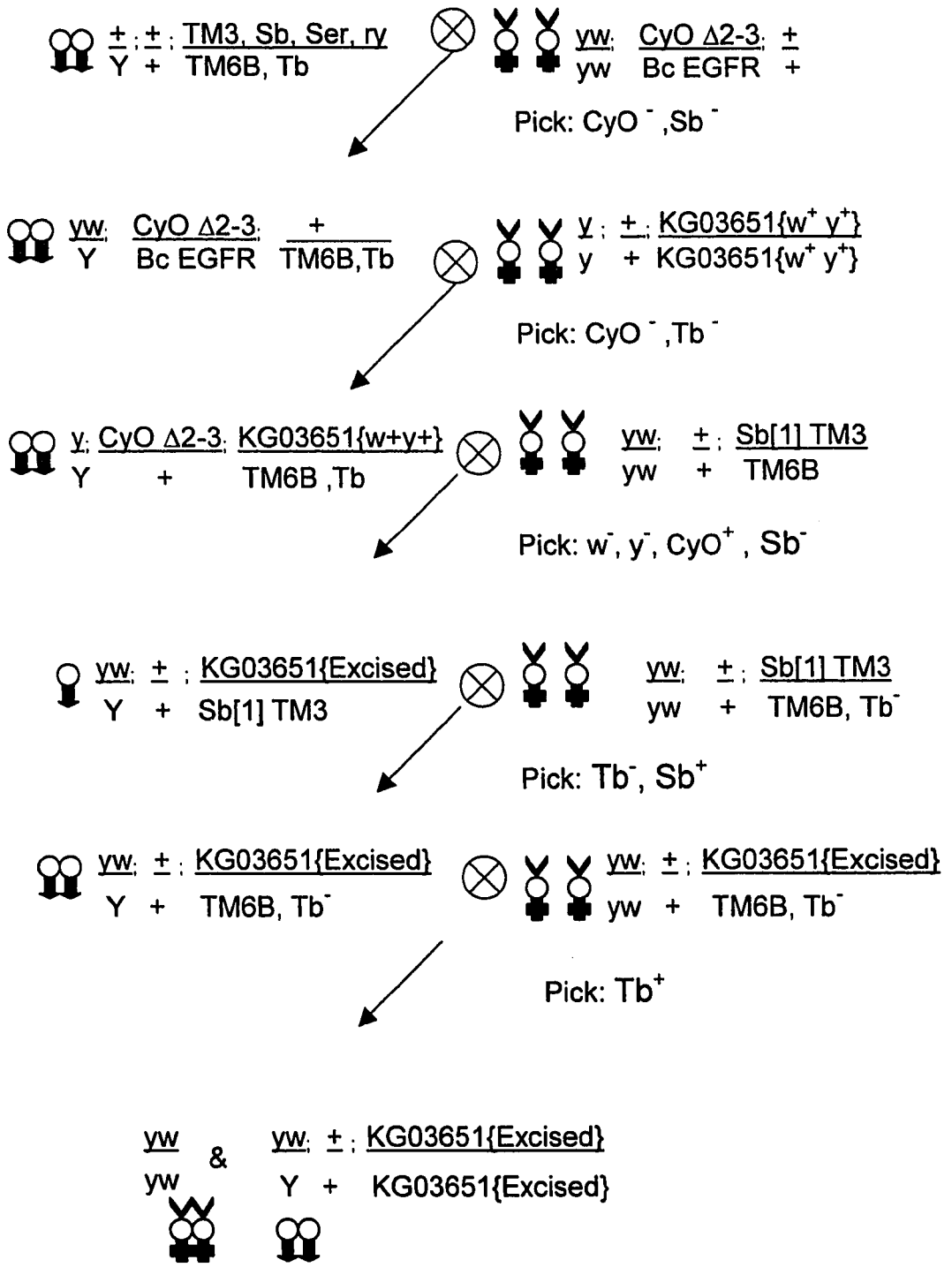

Figure 2.3 Excision of the *dunc-115 P* insertion. The *dunc-115 P* insertion (KG03651) was excised by crossing with a strain carrying a trangene encoding the transposase that mobilizes the *P* element. The absence of the *P* insertion was score by picking flies will yellow bodies and white eyes. Ultimately homozygous stocks were established.

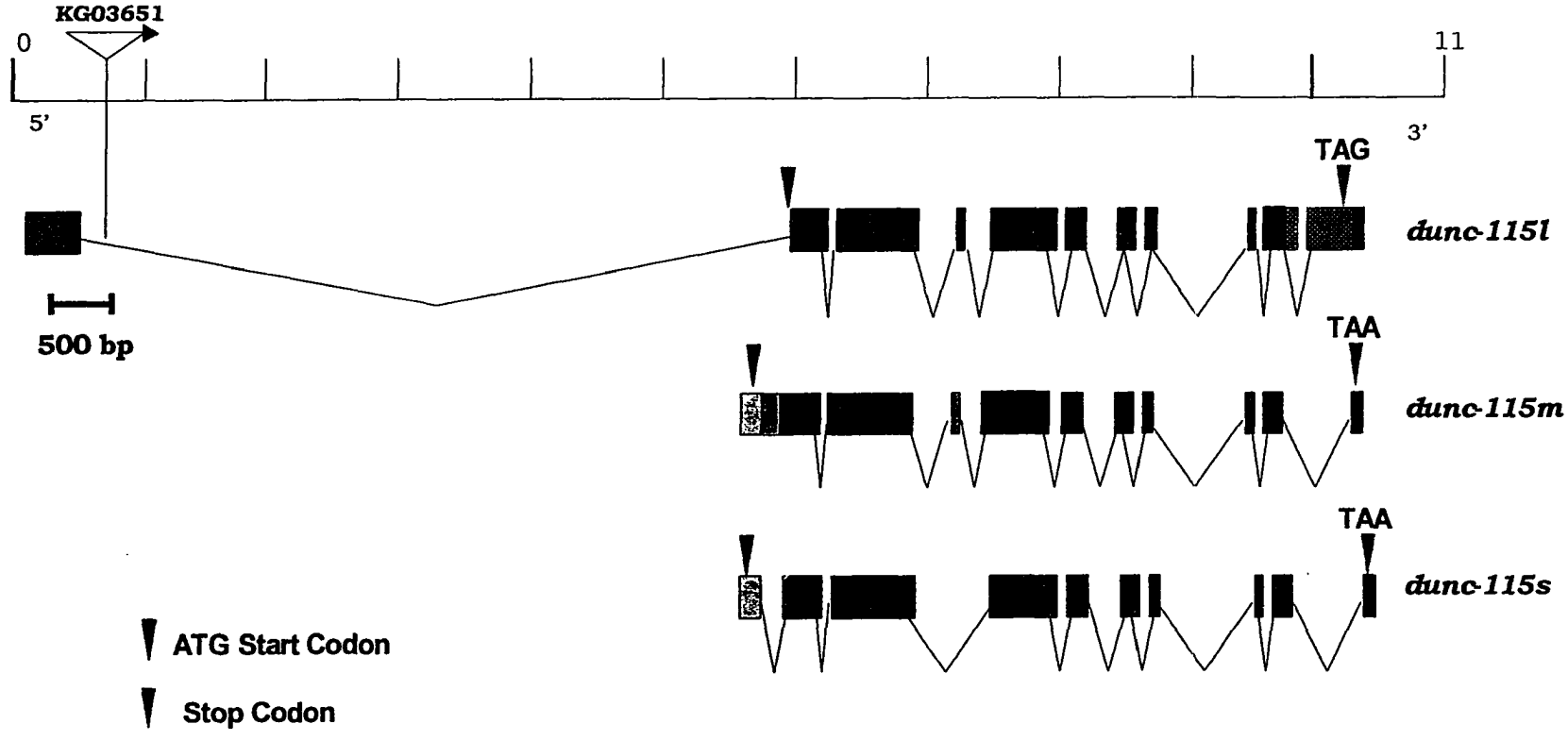

Figure 3.1 Map of *dunc-115* isoforms
Depicted here is the intron/exon structure of the three alternatively spliced isoforms of *dunc-115.* The gene spans approximately 10.7 Kb of the 3rd chromosome and the cDNA length for each isoform *dunc-115l*, *dunc-115m*, and *dunc-115s,* are 3.3kb, 2.7, and 2.4 respectively.

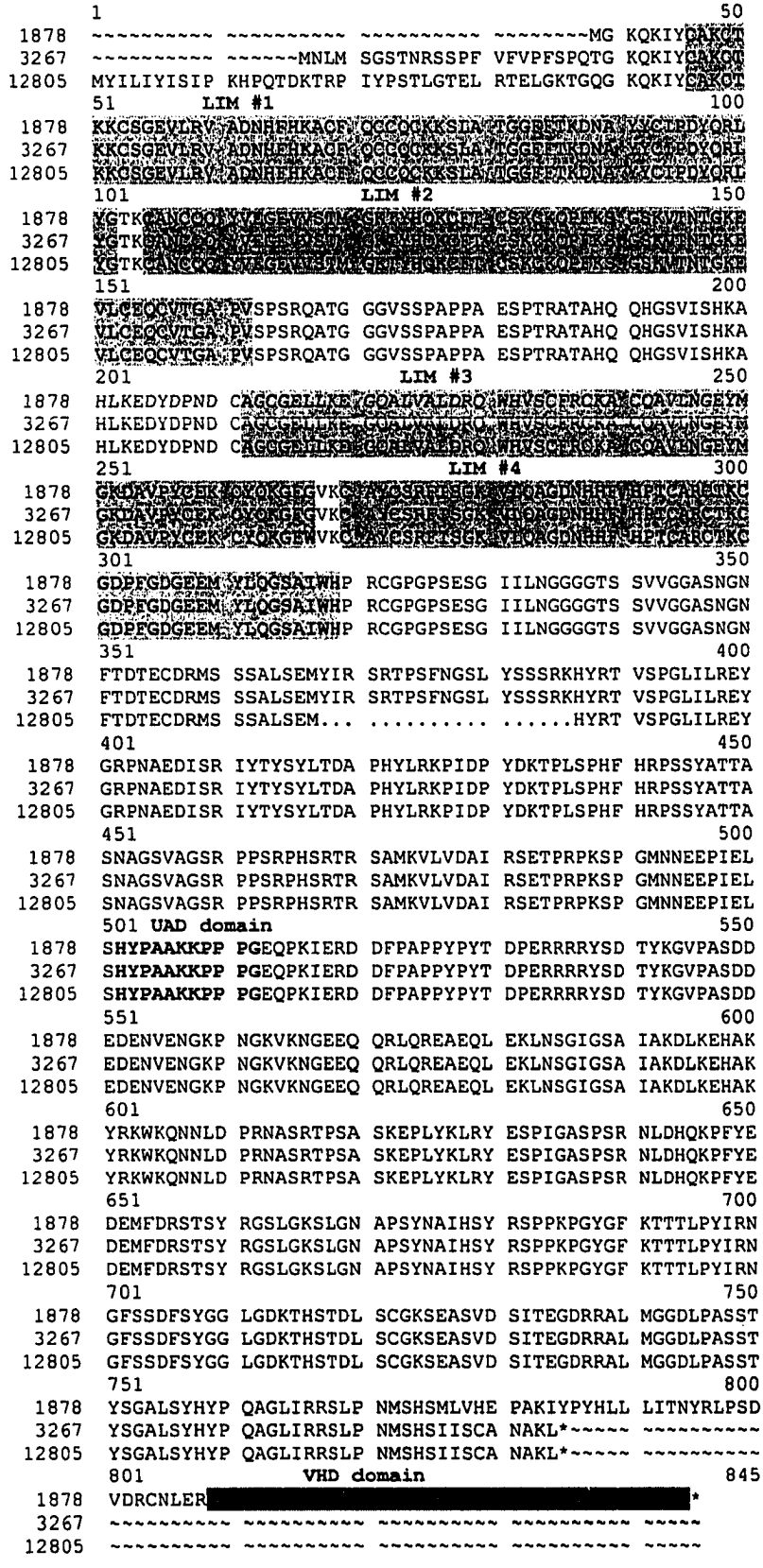

Figure 3.2 Comparison of the three Dunc-115 isoforms
The three cDNAs isolated encode three different isofoms. The functional domains are indicated.

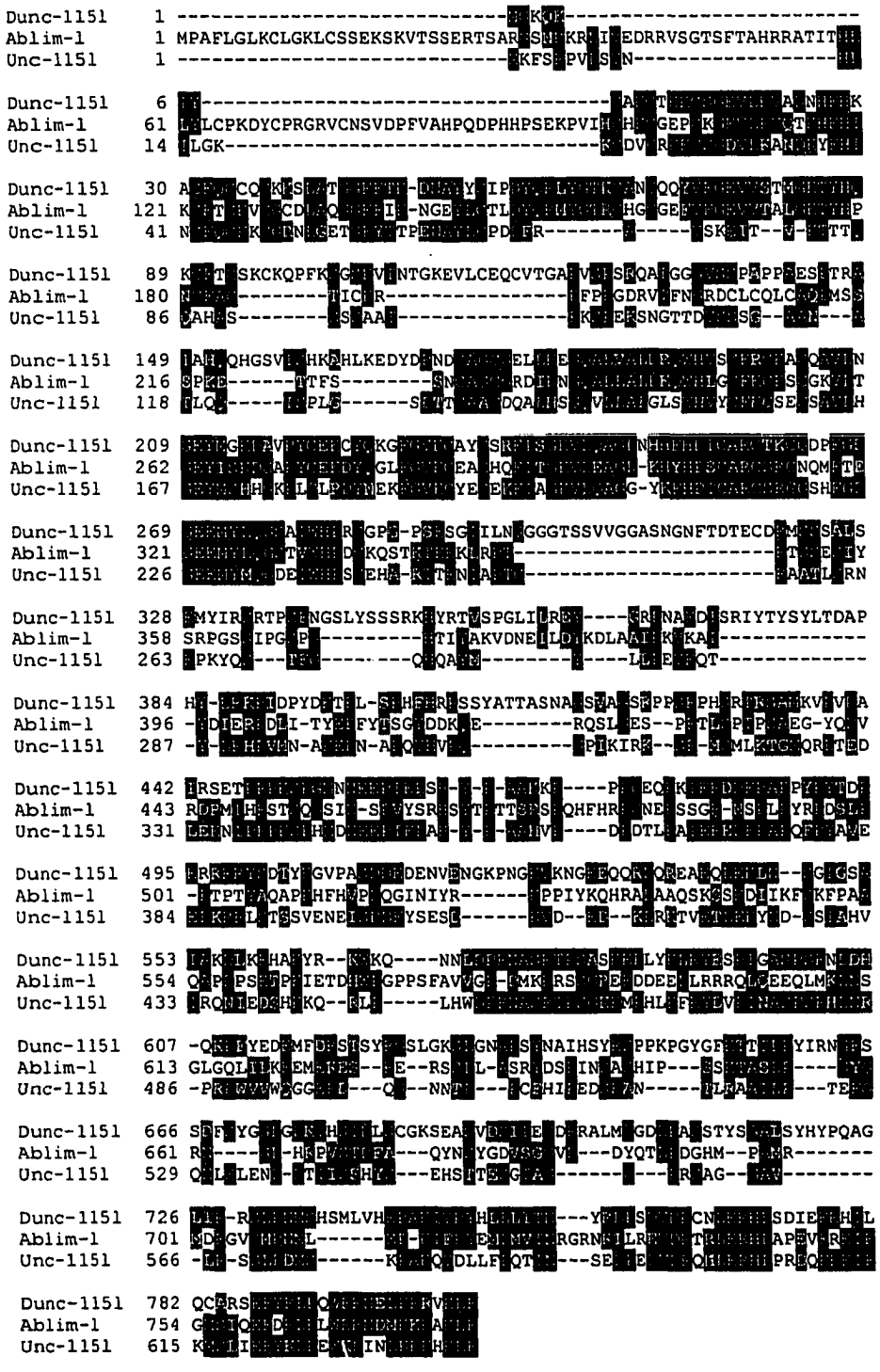

Figure 3.4 Conservation analysis between long isoforms of the orthologs.
Shown here are the long forms of Dunc-115, AbLIM, and UNC-115 The black shaded regions are identical amino acids and grey areas are the similar amino acids.

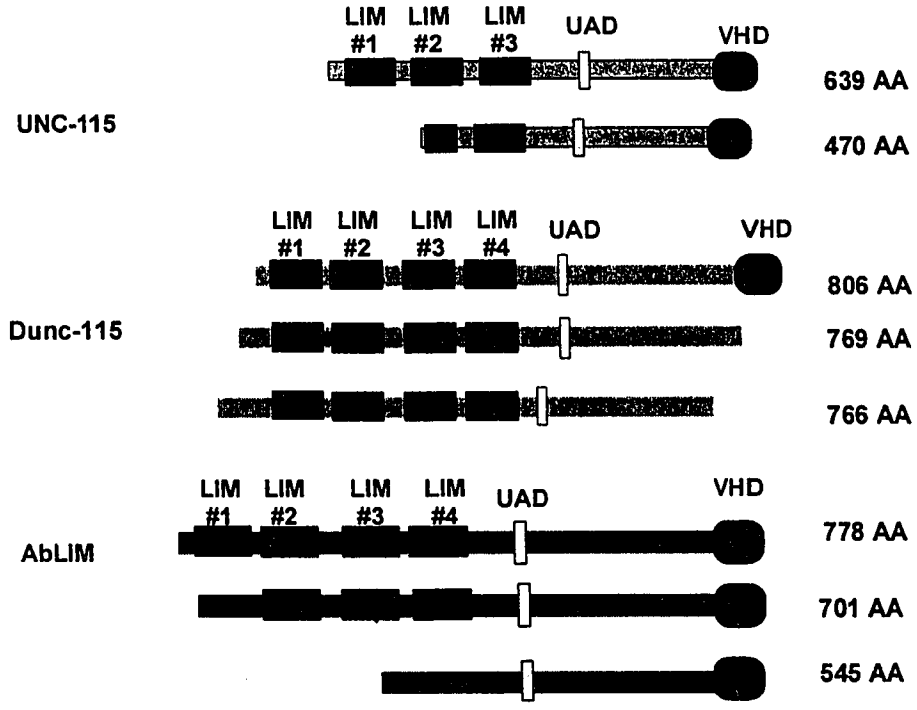

Figure 3.4 The of Dunc-115 and its orthologs
Depicted here is an illustration of Dunc-115 and its orthologs, AbLIM and UNC-115. Like their orthologs Dunc-115 encodes the LIM functional domain. LIM domains have been shown to play a role in protein-protein interaction. Additonally, they have a UAD, which has an unknown function but is characteristic of this family of proteins. Bioinformatic analysis shows only Dunc-115l contains a villin headpiece domain, while in the case of the orthologs all isoforms contain villin headpiece domains. Therefore, it appears that Dunc-115 m and s are novel family members.

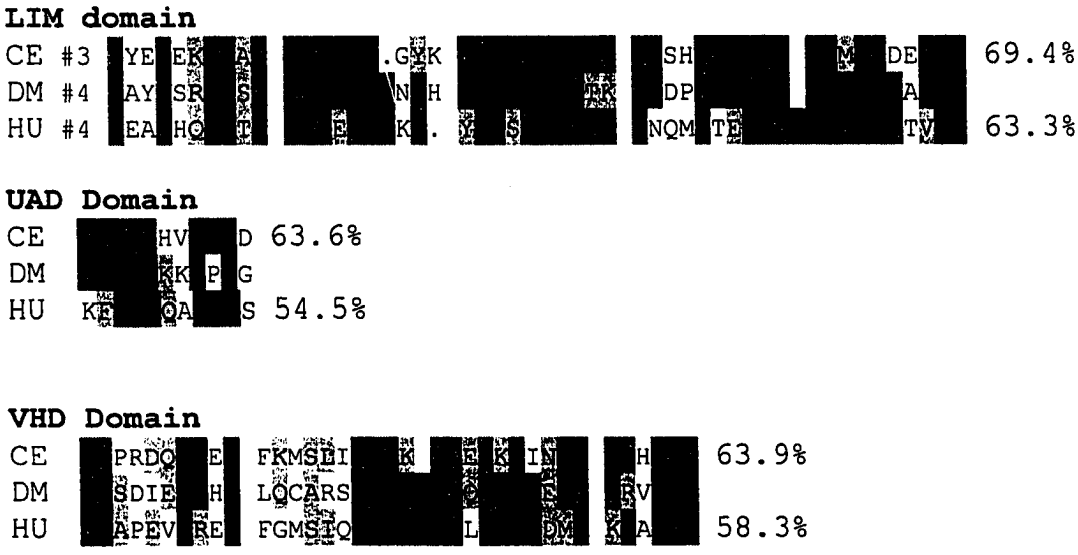

Figure 3.5 Conservation between LIM, UAD, and VHD domains.

LIM domains function in protein-protein interaction and Villin headpiece domains (VHD) function in binding actin. The function of the UAD domain is unknown but is present in UNC-115, AbLIM and Dematin. Both the LIM and VHD functional domains exhibit substantial conservation indicating that Dunc-115l (DM) may function similar to abLIM-l (HU) and UNC-115 (CE).

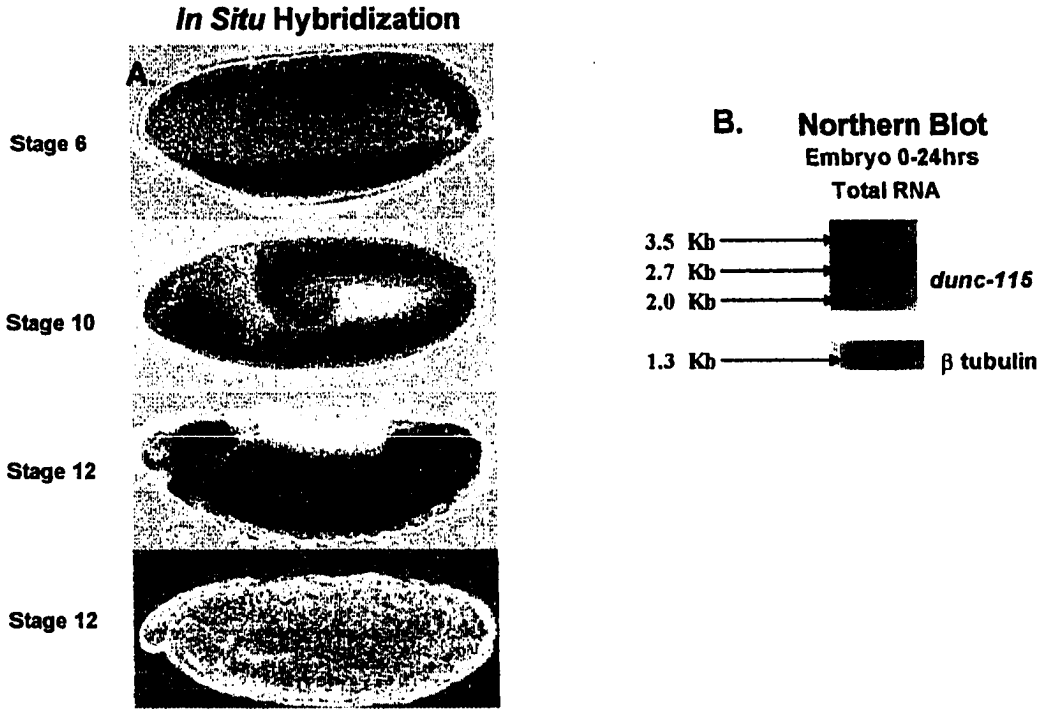

Figure 3.6 Expression analysis of *dunc-115*
(A) *In situ* hybridization during different stages of embryogenesis shows a dominance of *dunc-115* localization to the developing CNS and gut during stage 12. The bottom panel is the negative control. (B) The Northern blot shows diffuse bands. The arrows indicate the very top limit of the diffuse region and the bottom arrow defines the very bottom limit of the band. The middle arrow is the middle of between the two limits. This diffuse band indicates multiple isoforms for dunc-115 and is consistent with the cDNA sizes based on band

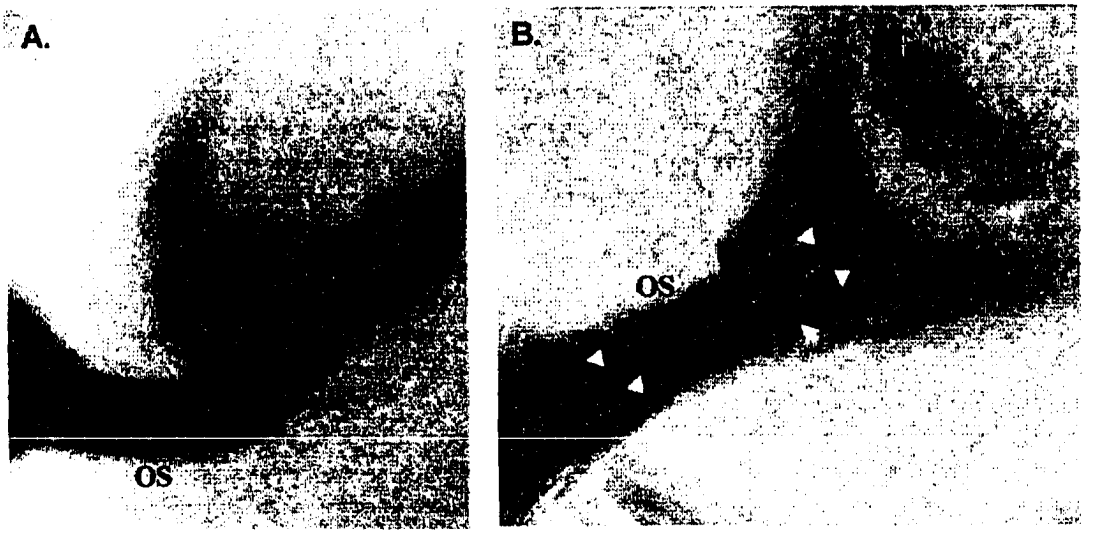

Figure 4.1 Investigation of photoreceptor projections in *dunc-115* mutants

The photoreceptor neuronal marker 24B10 was used investigate wild-type and *dunc-115* projections. (A) In wild type third instar larval photoreceptor axons project through the optic stalk (OS) and fan out to form the lamina plexis (LP) (B) *dunc-115* mutants exhibit failure to defasciculate causing gaps (arrowheads) and a folding-like phenotype (arrow). Additionally, there are abnormal crossovers of bundles (arrowheads).

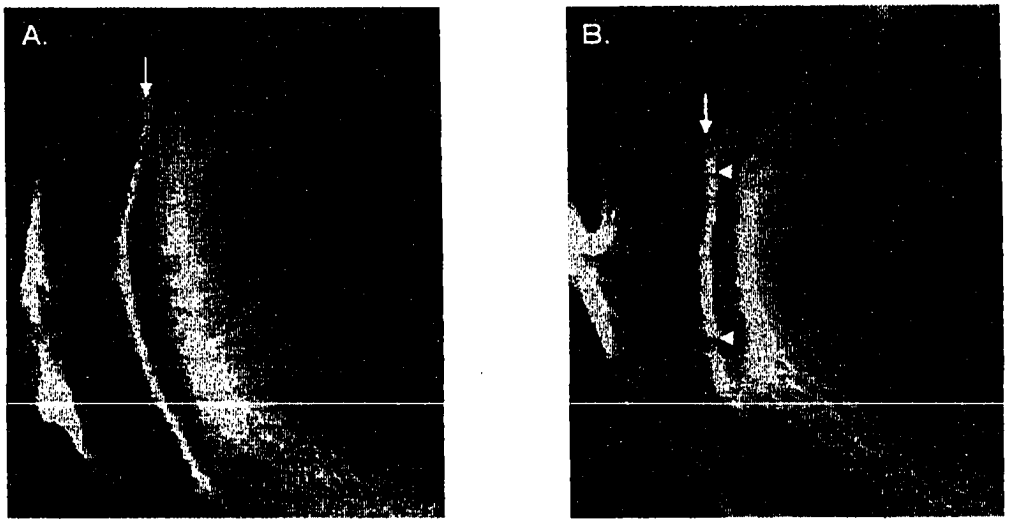

Figure 4.2 Investigation of *dunc-115* lamina target region

The third instar larva was stained with the pan neural FITC conjugated anti-HRP. (A) In wild-type we see a continuous crescent shaped lamina plexis. (B) *dunc-115* mutant exhibit gaps in the lamina plexis as indicated by the arrowheads

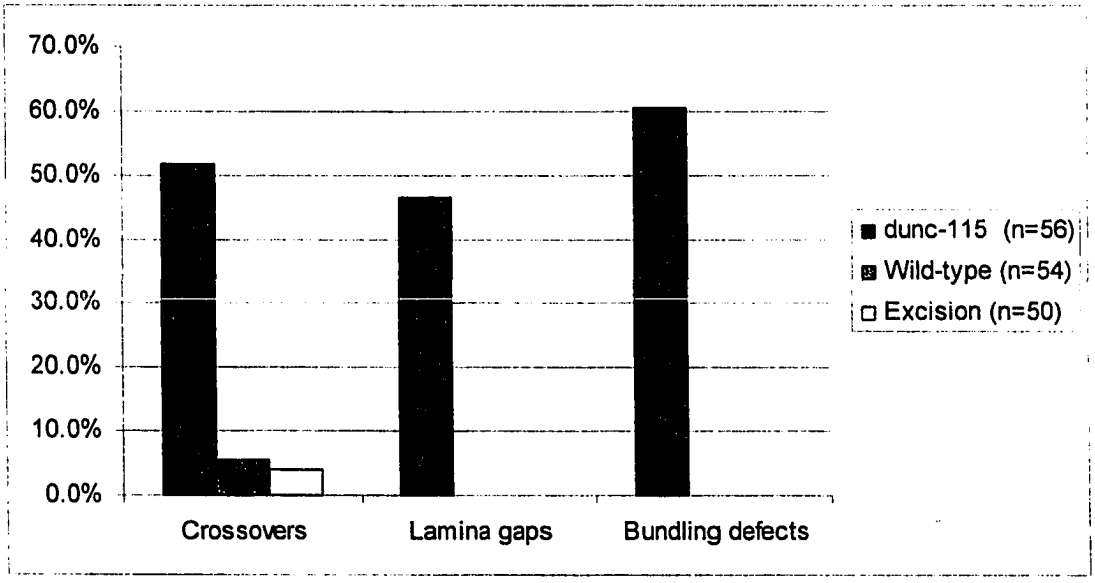

Figure 4.3 Quantitation of visual system defects
The visual system defects in *dunc-115* occur at a higher frequency than the wild type and excision strains. Analysis of the visual system showed three main defects; crossovers, gaps in the lamina and bundling defects. Crossovers were determined as two or more axons crossing over each other per specimen. Bundling defects were scored as folding of, gaps between and thickening of axon bundles.

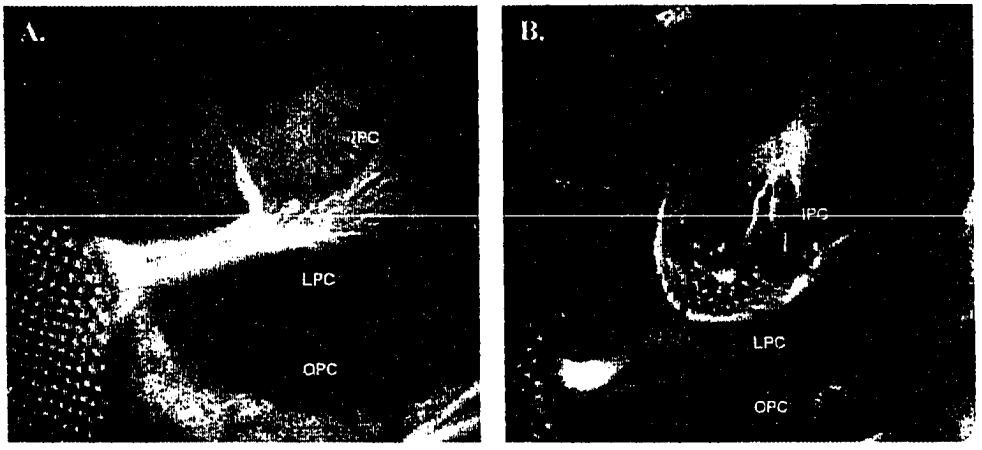

Figure 4.4 Investigation of cell division in *dunc-115* mutants

BrdU analysis was used to investigate if *dunc-115* influences cell division. FITC conjugated anti-HRP was used to visualize the neuronal projections. (A) In Canton S three proliferation centers are demarcated by BrdU, the outer proliferation center (OPC), lamina proliferation center (LPC) and inner proliferation center (IPC) (B) In *dunc-115* all three layers have are clearly demarcated. Indicating that dunc-115 does not influence cell division.

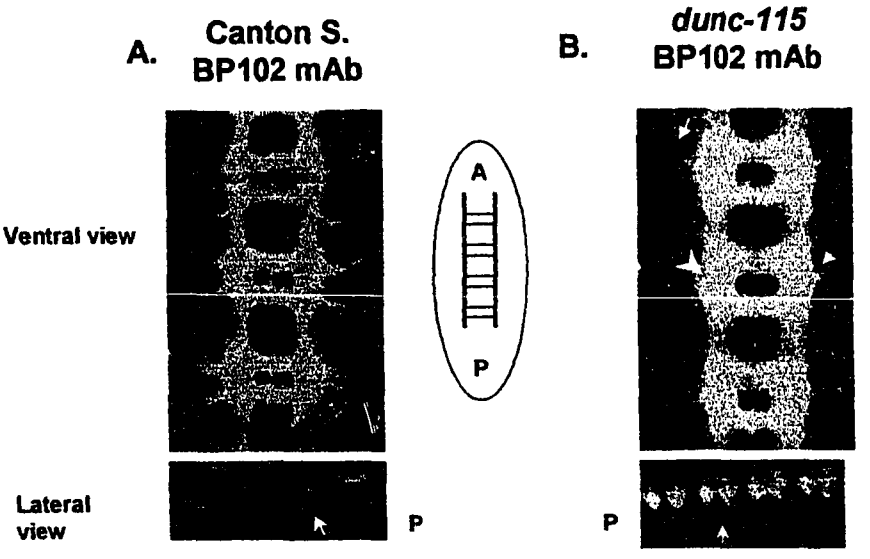

Figure 5.1 Investigation of midline projections in *dunc-115* mutants

An antibody that specifically marks midline projections, anti-BP102, was used to investigate if *dunc-115* affects midline axon pathfinding. (A) The wild type ventral view (top panel) shows the characteristic ladder like morphology of the midline formed by longitudinal and commissural projections. The SN and ISN projections exhibit a consistent pattern. The lateral view (bottom panel) shows the evenly spaced neuromeres (arrow). (B) A ventral view of the *dunc-115* mutants (top panel) exhibit thickening of the longitudinal bundles (arrowheads) as well as branching errors in the SN projections (arrows). The lateral prospective shows abnormal spacing of neuromeres in comparision to the wild type

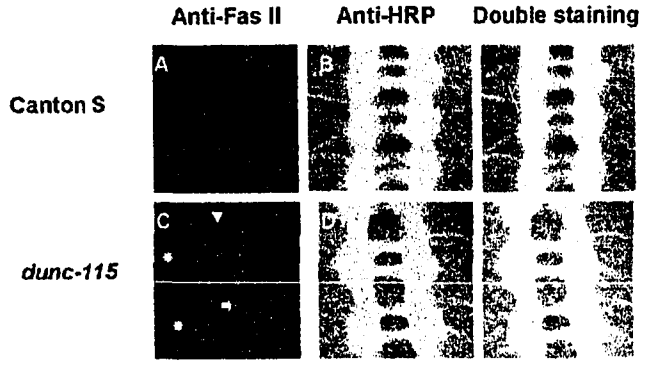

Figure 5.2 Investigation of longitudinal projections in *dunc-115* mutants

Wild type and *dunc-115* mutants were double stained with anti-Fas II and anti-HRP. (A) The Fas staining wild type midline exhibit three evenly spaced continuous parallel bundles that run lateral to the midline. (B) The anti-HRP staining midline shows the characteristic ladder-like shape. The Double staining panel shows that a subset of longitudinal axons are Fas II marked. (C) The anti-Fas II *dunc-115* mutants exhibit breaks (*) in the longitudinal bundles, defasciculation defects (arrow) and abnormal midline crossing of Fas II staining bundles. (D) The anti-HRP *dunc-115* midline exhibits thickness of longitudinal bundles and SN projection defects. The double staining panel shows that the breaks and defasciculation defects over lap with the thickened longitudinal bundles.

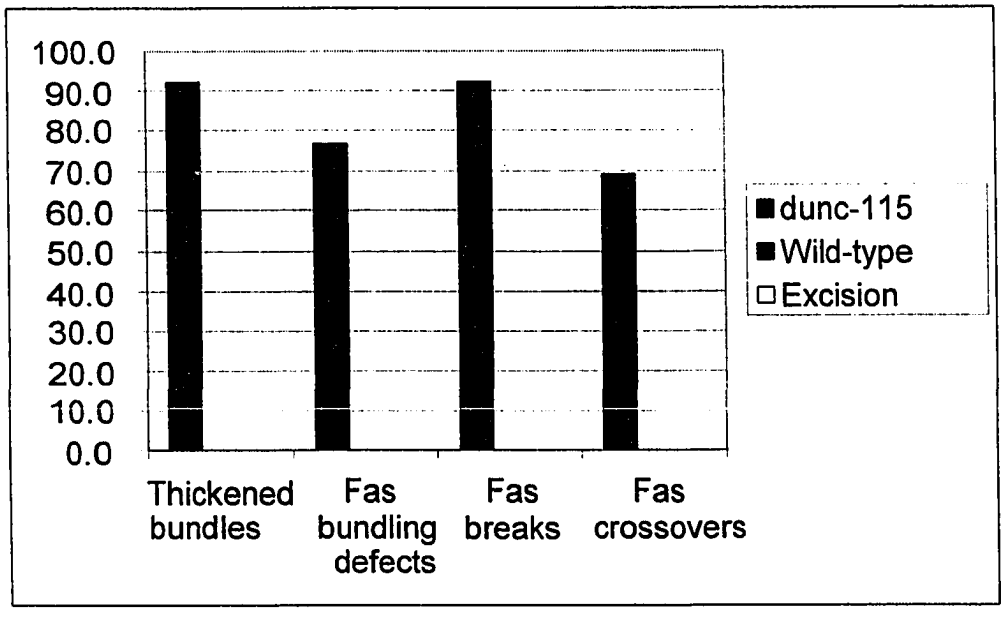

Figure 5.3 Quantitation of midline defects
The defects at the midline in *dunc-115* were observed. In contrast no defects were identified in wild type and the excision strains. Analysis of the midline when stained with BP102 or anti-HRP showed thickening of the longitudinal bundles. Staining with anti-Fas II exhibited bundling defects, breaks in the tracts and abnormal crossing over of Fas II staining axons

References

Reference List

Aberle,H., Haghighi,A.P., Fetter,R.D., McCabe,B.D., Magalhães,T.R., and Goodman,C.S. (2002). *wishful thinking* encodes a BMP type II receptor that regulates synaptic growth in *Drosophila*. Neuron *33*, 545-558.

Ackerman,S.L. and Knowles,B.B. (1998). Cloning and mapping of the UNC5C gene to human chromosome 4q21-q23. Genomics *52*, 205-208.

Albright,T.D., Jessel,T.M., Kandel,E.R., and Posner,M.I. (2000). Neural science: a century of progress and the mysteries that remain. Cell *25*, S1-S55.

Ashburner,M. (1989). Drosophila: *A laboratory manual.* (Cold Spring Harbor: Cold Spring Harbor Press).

Aspenström,P. (1999). Effectors for the Rho GTPases. Current Opinion in Cell Biology *11*, 95-102.

Awasaki,T., Saito,M., Sone,M., Suzuki,E., Sakai,R., Ito,K., and Hama,C. (2000). The *Drosophila* Trio plays an essential role in patterning of axons by regulating their directional extension. Neuron *26*, 119-131.

Bach,I. (2000). The LIM domain: regulation by association. Mechanisms of Development *91*, 5-17.

Bentley D. and Toroian-Raymond A. (1986). Disoriented pathfinding by pioneer neurone growth cones deprived of filopodia by cytochalasin treatment. Nature *323*, 712-5.

Bateman,J., Shu,H., and Vactor,D.V. (2000). The guanine nucleotide exchange factor Trio mediates axonal development in the *Drosophila* embryo. Neuron *26*, 93-106.

Bateman,J. and Van Vactor,D. (2001). The Trio family of guanine-nucleotide-exchange factors: regulators of axon guidance. Journal of Cell Science *114*, 1973-1980.

Borisy,G.G. and Svitkina,T.M. (2000). Actin machinery: pushing the envelope. Current Opinion in Cell Biology *12*, 104-112.

Bottalico,A.G., Garcia,M.C., Edwards,K., and He,Q. (2003). A role for gene *dizzy* in the visual system development of *Drosophila melanogaster.* Gene *Submitted.*

Brose,K. and Tessier-Lavigne,M. (2000). Slit proteins: key regulators of axon guidance, axonal branching, and cell migration. Curr. Opin. Neurobiol. *10*, 95-102.

Cant,K., Knowles,B.A., Miklos-Mahajan,S., Heintzelman,M., and Cooley,L. (1998). *Drosophila* fascin mutants are rescued by overexpression of the villin-like protein, quail. Journal of Cell Science *111*, 213-221.

Certel,S.J., Clyne,P.J., Carlson,J.R., and Johnson,W.A. (2000). Regulation of central neuron synaptic targeting by the *Drosophila* POU protein, Acj6. Development *127*, 2395-2405.

Chan,S.S.Y., Zheng,H., Su,M.W., Wilk,R., Killeen,M.T., Hedgecock,E.M., and Culotti,J.G. (1996). UNC-40 a *C. elegans* homolog of DCC (deleted in colorectal cancer), is required in motile cells responding to UNC-6 netrin cues. Cell *87*, 187-195.

Clandinin,T.R. and Zipursky,S.L. (2002). Making connections in the fly visual system. Neuron *35*, 827-841.

Colamarino,S.A. and Tessier-Lavigne,M. (1995). The axonal chemoattractant netrin 1 is also a chemorepellent for trochlear motor axons. Cell *81*, 621-629.

Cooper,J.A. and Schafer,D.A. (2000). Control of actin assembly and disassembly at filament ends. Current Opinion in Cell Biology *12*, 97-103.

David,V., Gouin,E., Troys,M.V., Grogan,A., Segal,A.W., Ampe,C., and Cossart,P. (1998). Identification of cofilin, coronin, Rac and capZ in actin tails using a Listeria affinity approach. Journal of Cell Science *111*, 2877-2884.

Dearborn,R., Jr., He,Q., Kunes,S., and Dai,Y. (2002). Eph receptor tyrosine kinase-mediated formation of a topographic map in the Drosophila visual system. J. Neurosci. *22*, 1338-1349.

de la Torre J.R., Hopker V.H., Ming G.L., Poo M.M., Tessier-Lavigne M., Hemmati-Brivanlou A., and Holt C.E. (1997). Turning of retinal growth cones in a netrin-1 gradient mediated by the netrin receptor DCC. Neuron *19*, 1211-24.

Dickson,B. and Hafen,E. (1993). Genetic dissection of eye development in *Drosophila*. In The Development of *Drosophila Melanogaster*, M.Bate and A.M.Arias, eds. (Cold Spring Harbor: Cold Spring Harbor Press), pp. 1327-1362.

Dickson,B.J. (2001). Rho GTPases in growth cone guidance. Current Opinion in Neurobiology *11*, 103-110.

Dickson,B.J. and Keleman,K. (2002). Netrins. Current Biology *12*, R154-R155.

Dickson,B.J. (2002). Molecular mechansims of axon guidance. Science *298*, 1959-1964.

Dickson,B.J. and Senti,K.A. (2002). Axon guidance: growth cones make an unexpected turn. Curr. Biol. *12*, R218-R220.

Dirks,P.B. (2001). Glioma migration: clues from the biology of neural progenitor cells and embryonic CNS cell migration. J. Neurooncol. *53*, 203-212.

Erkman,L., Yates,P.A., McLaughlin,T., McEvilly,R.J., Whisenhunt,T., O'Connell,S.M., Krones,A.I., Kirby,M.A., Rapaport,D.H., Bermingham,J.R., O'Leary,D.D.M., and Rosenfeld,M.G. (2000). A POU domain transcription factor-dependent program regulates axon pathfinding in the vertebrate visual system. Neuron *28*, 779-792.

Ferrary,E., Cohen-Tannoudji,M., Pehau-Arnaudet,G., Lapillonne,A., Athman,R., Ruiz,T., Boulouha,L., El Marjou,F., Doye ,A., Fontaine,J.J., Antony,C., Babinet,C., Louvard,D., Jaisser,F., and Robine,S. (1999). In vivo, villin is required for Ca(2+)-dependent F-actin disruption in intestinal brush borders. Journal of Cell Biology *146*, 819-830.

Friederich,E., Vancompernolle,K., Louvard,D., and Vandekerckhove,J. (1999). Villin function in the organization of the actin cytoskeleton: correlation of *in vivo* effects to it biochemical activities in vitro. The Journal of Biological Chemistry *274*, 26751-26760.

Garcia,M.C. and He,Q. (2003). Identification and characterization of a novel *Drosophila* gene *dunc-115*. Mechanisms of Development *Submitted*.

Giger,R.J. and Kolodkin,A.L. (2000). Frazzled precision guides axons. Nature *406*, 841-843.

Gitai,Z., Yu,T.W., Lundquist,E.A., Tessier-Lavigne,M., and Bargmann,C.I. (2003). The Netrin receptor UNC-40/DCC stimulates axon attraction and outgrowth through Enabled and in parallel, Rac and UNC-115/ABLIM. Neuron *37*, 53-65.

Goda,Y. (2002). Cadherins communicate structural plasticity of presynaptic and postsynaptic terminals. Neuron *35*, 1-7.

Goodman,C.S. and Doe,C.Q. (1993). Embryonic development of the *Drosophila* central nervous system. In The Development of *Drosophila melanogaster*, M.Bate and A.M.Arias, eds. (Plainview: Cold Spring Harbor Laboratory Press), pp. 1131-1206.

Goodman,C.S. and Shatz,C.J. (1993). Developmental mechanisms that generate precise patterns of neuronal connectivity. Cell *72 Suppl*, 77-98.

Greenspan,R.J. (1997). Fly Pushing. (Cold Spring Harbor: Cold Spring Harbor Laboratory Press), pp. 12-14.

Guthrie,S. (1999). Axon guidance: starting and stopping with slit. Current Biology *9*, R432-R435.

Harris,R., Sabatelli,L.M., and Seeger,M.A. (1996). Guidance cues at the Drosophila CNS midline: identification and characterization of two Drosophila Netrin/Unc-6 homologs. Neuron *17*, 217-228.

Hayden,S.M., Miller,P.S., Brauweiler,A., and Bamburg,J.R. (1993). Analysis of the interactions of actin depolymerizing factor with G- and F- actin. Biochemistry *32*, 9994-1004.

He,Q. (2000). A functional analysis of the involvement of cytoskeleton proteins in *Drosophila* visual system. Methods in Molecular Biology *161*, 279-283.

Hedgecock,E.M., Culotti,J.G., and Hall,D.H. (1990). The unc-5, unc-6, and unc-40 genes guide circumferential migrations of pioneer axons and mesodermal cells on the epidermis in C. elegans. Neuron *4*, 61-85.

Hidalgo,A. and Booth,G. (2000). Glia dictate pioneer axon trajectories in the *Drosophila* embryonic CNS. Development *127*, 393-402.

Hing,H., Xiao,J., Harden,N., Lim,L., and Zipursky,S.L. (1999). Pak functions downstream of Dock to regulate photoreceptor axon guidance in Drosophila. Cell *97*, 853-863.

Hong K., Hinck L., Nishiyama M., Poo M. M., Tessier-Lavigne M., and Stein E. (1999). A ligand-gated association between cytoplasmic domains of UNC5 and DCC family receptors converts netrin-induced growth cone attraction to repulsion. Cell *97*, 927-41.

Huang,Z. and Kunes,S. (1996). Hedgehog, transmitted along retinal axons, triggers neurogenesis in the developing visual centers of the Drosophila brain. Cell *86*, 411-422.

Hug,C., Jay,P.Y., Reddy,I., McNally,J.G., Bidgman,P.C., Elson,E.L., and Cooper,J.A. (1995). Capping protein levels influence actin assembly and cell motility in *Dictyostelium*. Cell *81* , 591-600.

Hummel,T., Schimmelpfeng,K., and Klämbt,C. (1999). Commissure formation in the embryonic CNS of Drosophila. Developmental Biology *209*, 381-398.

Kaphingst,K. and Kunes,S. (1994). Pattern formation in the visual centers of the Drosophila brain: wingless acts via decapentaplegic to specify the dorsoventral axis. Cell *78*, 437-448.

Kaprielian,Z., Runko,E., and Imondi,R. (2000). Axon guidance at the midline of developing CNS. The Anatomical Record *261*, 176-197.

Kaprielian,Z., Runko,E., and Imondi,R. (2001). Axon guidance at the midline choice point. Dev. Dyn. *221*, 154-181.

Keleman,K. and Dickson,B.J. (2001). Short- and long-range repusion by the *Drosophila* Unc5 netrin receptor. Neuron *32*, 605-617.

Kennerdell,J.R. and Carthew,R.W. (2001). Heritable gene silencing in *Drosophila* using double-stranded RNA. Nature Biotechnology *18*, 896-898.

Kidd,T., Bland,K.S., and Goodman,C.S. (1999). Slit is the midline repellent for the robo receptor in *Drosophila*. Cell ***96***, 785-794.

Kolodziej,P.A., Timpe,L.C., Mitchell,K.J., Fried,S.R., Goodman,C.S., Jan,L.Y., and Jan,Y.N. (1996). *frazzled* encodes a drosophila member of the DCC immunoglobuling subfamily and is required for CNS and motor axon guidance. Cell *87*, 197-204.

Kunes,S., Wilson,C., and Steller,H. (1993). Independent guidance of retinal axons in the developing visual system of Drosophila. J. Neurosci. *13*, 752-767.

Lam,G. and Thummel,C.S. (2000). Inducible expression of double-stranded RNA directs specific genetic interference in *Drosophila* . Current Biology *10*, 957-963.

Landgraf,M., Bossing,T., Technau,G.M., and Bate,M. (1997). The origin, location, and projections of the embryonic abdominal motorneurons of *Drosophila*. The Journal of Neuroscience *17*, 9642-9655.

Lanier,L.M. and Gertler,F.B. (2000). From Abl to actin: Abl tyrosine kinase and associated proteins in growth cone motility. Current Opinion in Neurobiology *10*, 80-87.

Lee,J.D. and Treisman,J.E. (2001). The role of Wingless signaling in establishing the anteroposterior and dorsoventral axes of the eye disc. Development *128*, 1519-1529.

Lee, C.H., Herman, T., Clandinin, T.R., Lee, R., Zipursky, S.L. (2001). N-cadherin regulates target specificity in the Drosophila visual system. Neuron *30*, 437-50.

Lee, Y. S. and Carthew, R. W. Making a better RNAi vector for *Drosophila*: use of intron spacers. Methods in press. 2002.

Lewis, A. K. and Bridgman, P. C (1992). Nerve growth cone lamellipodia contain two populations of actin filaments that differ in organization and polarity. Journal of Cell Biology *119*, 1219-43.

Liao,G., Rehm,E.J., and Rubin,G.M. (2000). Insertion site preference of the P transposable element in *Drosophila melanogaster*. Proceedings of the National Academy of Sciences, USA *97*, 3347-3351.

Liebl,E., Forsthoefel,D.J., Franco,L.S., Sample,S.H., Hess,J.E., Cowger,J.A., Chandler,M.P., Shupert,A.M., and Seeger,M.A. (2000). Dosage-sensitive, reciprocal genetic interactions between the *Abl* tyrosine kinase and the Putative GEF *trio* reveal *trio's* role in axon pathfinding. Neuron *26*, 107-118.

Lin,M.Z. and Greenberg,M.E. (2000). Orchestral maneuvers in the axon: Trio and the control of axon guidance. Cell *101*, 239-242.

Loisel,T.P., Boujemaa,R., Pantaloni,D., and Carlier,M. (1999). Reconstitution of actin-based motility of Listeria and Shigella using pure proteins. Nature *401*, 613-616.

Lum L., Yao S., Mozer B., Rovescalli A., Von Kessler D., Nirenberg M., and Beachy PA. (2003). Identification of Hedgehog pathway components by RNAi in Drosophila cultured cells. Science *299*, 2039-45.

Lundquist,E.A., Herman,R.K., Shaw,J.E., and Bargmann,C.I. (1998). UNC-115, a conserved protein with predicted LIM and actin-binding domains mediates axon guidance in *C. elegans*. Neuron *21*, 385-392.

Luo,L. (2000). Trio Quartet in D. (melanogaster). Neuron *26*, 1-4.

Luo,L., Jan,L.Y., and Jan,Y.J. (2000). Rho family small GTP-binding proteins in growth cone signalling. Current Opinion in Neurobiology *7*, 81-86.

Luo,L. (2000). Rho GTPases in neuronal morphogenesis. Nature Reviews Neuroscience *1*, 173-180.

Marks,P.W., Arai,M., Bandura,J.L., and Kwiatokowski,D.J. (1998). Advillin (p92): a new member of the gelsolin/villin family of actin regulatory proteins. Journal of Cell Science *111*, 2129-2136.

Mitchell,K.J., Doyle,J.L., Serafini,T., Kennedy,T.E., Tessier-Lavigne,M., Goodman,C.S., and Dickson,B.J. (1996). Genetic analysis of *netrin* genes in drosophila: Netrins guide CNS commissural axons and peripheral motor axons. Neuron *17*, 203-215.

Mueller,B.K. (1999). Growth Cone Guidance: First steps towards a deeper understanding. Annual Reviews of Neuroscience *22*, 351-388.

Mullins,R.D., Heuser,J.A., and Pollard,T.D. (1998). The interaction of Arp2/3 complex with actin: nucleation, high affinity pointed end capping, and formation of branching networks of filaments. Proceedings of the National Academy of Sciences, USA *95*, 6181-6186.

Myers,E.W., Sutton,G.G., Delcher,A.L., Dew,I.M., Fasulo,D.P., Flanigan,M.J., Kravitz,S.A., Mobarry,C.M., Reinert,K.H., Remington,K.A., Anson,E.L., Bolanos,R.A., Chou,H., Jordan,C.M., Halpern,A.L., Lonardi,S., Beasley,E.M.,

Brandon,R.C., Chen,L., Dunn,P.J., Lai,Z., Liang,Y., Nusskern,D.R., Zhan,M., Zhang,Q., Zheng,X., Rubin,G.M., Adams,M., and Venter,C.J. (2000). A whole genome assembly of *Drosophila*. Science *287*, 2196-2204.

Newsome,T.P., Schmidt,S., Dietzl,G., Keleman,K., □sling,B., Debant,A., and Dickson,B.J. (2000). Trio combines with dock to regulate pak activity during photoreceptor axon pathfinding in *Drosophila*. Cell *101*, 283-294.

Okada,K., Obinata,T., and Abe,H. (1999). XAIP1: a *Xenopus* homologue of yeast actin interacting protein 1 which induces disassembly of actin filaments cooperatively with ADF/Cofilin family proteins. Journal of Cell Science *112*, 1553-1565.

Oldenbourg,R., Katoh,K., and Danuser,G. (2000). Mechanism of lateral movement of filopodia and radial actin bundles across neuronal growth cones. Biophysical Journal *78*, 1176-1182.

Patel,B.N. and Van Vactor,D. (2002). Axon guidance: the cytoplasmic tail. Current Opinion in Cell Biology *14*, 221-229.

Prehoda,K.E., Scott,J.A., Mullins,R.D., and Lim,W.A. (2000). Integration of multiple signals through cooperative regulation of the N-WASP-Arp2/3 complex. Science *290*, 801-806.

Ranscht,B. (2000). Cadherins: molecular codes for axon guidance and synapse formation. The International Journal of Developmental Neuroscience *18*, 643-651.

Rhee,J., Mahfooz,N.S., Arregui,C., Lilien,J., Balsamo,J., and VanBerkum,M.F.A. (2002). Activation of the repulsive receptor Roundabout inhibits N-cadherin-mediated cell adhesion. Nature Cell Biology *4*, 798-805.

Rochline, M. W., Dailey, M. E., and Bridgman, P. C. (1999). Polymerizing microtubules activate site-directed F-actin assembly in nerve growth cones. Molecular Biology of the Cell *10*, 2309-27.

Rohatgi,R., Ma,L., Miki,H., Lopez,M., Kirchhausen,T., Takenawa,T., and Kirschner,M.W. (1999). The interaction between N-WASP and the Arp2/3 complex links Cdc-42-dependent signals to actin assembly. Cell *97*, 221-231.

Roof,D.J., Hayes,A., Adamian,M., Chishti,A.H., and Li,T. (1997). Molecular characterization of abLIM, a novel actin-binding and double zinc finger protein. The Journal of Cell Biology *138*, 575-588.

Salecker,I., Clandinin,T.R., and Zipursky,S.L. (1998). Hedgehog and Spitz: making a match between photoreceptor axons and their targets. Cell *95*, 587-590.

Schmid,A., Schindelholz,B., and Zinn,K. (2002). Combinatorial RNAi: a method for evaluating the functions of gene families in *drosophila.* Trends in Neurosciences *25*, 71-74.

Senti,K., Keleman,K., Eisenhaber,F., and Dickson,B.J. (2000). *breakless* is required for lamina targeting of R1-6 axons in the *Drosophila* visual system. Development *127*, 2291-2301.

Serafini,T., Kennedy,T.E., Galko,M.J., Mirzayan,C., Jessell,T.M., and Tessier-Lavigne,M. (1994). The netrins define a family of axon outgrowth-promoting proteins homologous to C. elegans UNC-6. Cell *78*, 409-424.

Serafini,T., Colamarino,S.A., Leonardo,E.D., Wang,H., Beddington,R., Skarnes,W.C., and Tessier,L. (1996). Netrin-1 is required for commisural axon guidance in the developing vertebrate nervous system. Cell *87*, 1001-1014.

Small,J.V., Stradal,T., Vignal,E., and Rottner,K. (2002). The lamellipodium: where motility begins. Trends in Cell Biology *12*, 112-120.

Sperry, R. W. Chemoaffinity in the orderly growth of nerve fiber patterns and connections. Proceedings of the National Academy of Sciences, USA 50, 703-709. 1963.

Steketee,M.B. and Tosney,K.W. (2002). Three functionally distinct adhesions in filopodia: shaft adhesions control lamellar extension. The Journal of Neuroscience *22*, 8071-8083.

Steven,R., Kubiseski,T.J., Zheng,H., Kulkarni,S., Mancillas,J., Ruiz,M.A., Hogue,C.W., Pawson,T., and Culotti,J. (1998). UNC-73 activates the Rac GTPase and is required for cell and growth cone migrations in C. elegans. Cell *92*, 785-795.

Struckhoff,E.C. and Lundquist,E.A. (2003). The actin-binding protein UNC-115 is an effector of Rac signaling during axon pathfinding in *C. elegans*. Development *130*, 693-704.

Takenawa,T. and Miki,H. (2001). WASP and WAVE family proteins: key molecules for rapid rearrangement of cortical actin filaments and cell movement. Journal of Cell Science *114*, 1801-1809.

Tessier-Lavigne,M. and Goodman,C.S. (1996). The molecular biology of axon guidance. Science *274*, 1123-1133.

Theriot,J.A. (1997). Accelerating on treadmill: ADF/cofilin promotes rapid actin filament turnover in the dynamic cytoskeleton. Journal of Cell Biology *136*, 1165-1168.

Tower,J., Karpen,G.H., Craig,N., and Spradling,A.C. (1993). Peferential transposition of *Drosophila P* elements to nearby chromosomal sites. Genetics *133*, 347-359.

Török,T., Tick,G., Alvarado,M., and Kiss,I. (1993). *P-lacW* insertional mutagenesis on the second chromosome of *Drosophila melanogaster* : isolation of lethals with different overgrowth Phenotypes. Genetics *135*, 71-80.

Treisman,J.E. and Heberlein,U. (1998). Eye development in Drosophila: formation of the eye field and control of differentiation. Curr. Top. Dev. Biol. *39*, 119-158.

Wadsworth,W.G. (2002). Moving around in a worm: netrin UNC-6 and circumferential axon guidance in C. elegans. Trends Neurosci. *25*, 423-429.

Wolff,T. and Ready,D. (1993). Pattern formation in the Drosophila retina. In The Development of *Drosophila Melanogaster*, M.Bate and A.M.Arias, eds. (Cold Spring Harbor: Cold Spring Harbor Press), pp. 1277-1326.

Wolff,T., Martin,K.A., Rubin,G.M., and Zipursky,S.L. (1997). The development of the *Drosophila* visual system. In Molecular and Cellular Approaches to Neural Development, W.M.Cowan, T.M.Jessel, and S.L.Zipursky, eds. (New York: Oxford University Press), pp. 474-508.

Wong,K., Park,H.T., Wu,J.Y., and Rao,Y. (2002). Slit proteins: molecular guidance cues for cells ranging from neurons to leukocytes. Current Opinion in Genetics and Development *12*, 583-591.

Wood,W. and Martin,P. (2002). Structures in focus: filopodia. The International Journal of Biochemistry & Cell Biology *34*, 726-730.

Wu,Q. and Maniatis,T. (1999). A striking organization of a large family of human neural cadherin-like cell adhesion genes. Cell *97*, 779-790.

Zhang,P. and Spradling,A.C. (1993). Efficient and dispersed local *P* element transposition from *Drosophila* females. Genetics *133*, 361-373.

Zheng JQ, Wan JJ, and Poo MM. (1996). Essential role of filopodia in chemotropic turning of nerve growth cone induced by a glutamate gradient. Journal of Neuroscience *16*, 1140-9.

Zhen,H. and Kunes,S. (1998). Hedgehog, transmitted along retinal axons, triggers neurogenesis in the developing visual centers of the *Drosophila* brain. Cell *95*, 693-703.

Zipursky S. L., Venkatesh T. R., Teplow D. B., and Benzer S. (1984). Neuronal development in the Drosophila retina: monoclonal antibodies as molecular probes. Cell *36*, 15-26.